Infectious Atypical Pneumonia

20

Lianchun Liang

Infectious atypical pneumonia, also known as severe acute respiratory syndrome (SARS), is an acute respiratory infectious disease caused by SARS coronavirus (SARS-CoV). Clinically, it is characterized by fever, headache, muscular soreness, fatigue, dry cough rarely with phlegm, and diarrhea. Most patients experience accompanying pneumonia. In severe cases, the conditions may develop into acute lung injury, acute respiratory distress syndrome (ARDS), or even multiple organ failure that causes death. In China, SARS has been legally listed as one of the class B infectious diseases but is managed as class A infectious diseases, like anthrax and human infection of avian influenza.

20.1 Etiology

The pathogenic microorganism of SARS is the novel variant coronavirus, SARS coronavirus (SARS-CoV), whose gene is different from the known three groups of classic coronavirus. After its infection, the antibody produced in the human body is different from the antibodies produced after infection of the known three groups of coronavirus. These differences indicate that SARS-CoV is a novel pathogenic virus to humans. Based on previous knowledge, three groups (group 1, group 2, and group 3) of coronavirus and three serotypes (HcoV-229E of group 1 and HCoV-OC43 of group 2) are identified. At present, SARS-CoV is identified as group 4 of coronavirus.

SARS-CoV is an enveloped virus and is categorized under the genus *Betacoronavirus* and family *Coronaviridae*. Its diameter is commonly 60–120 mm, with radially arranged petal or cilium-like protrusions on its envelope. The protrusion is about 20 mm in length or longer with a narrow base and with a crown-like appearance resembling the classic coronavirus. The viral envelope mainly includes three types of glycoproteins: spike protein (S protein), membrane protein (M protein), and envelope protein (E protein). In some viral strains, hemagglutinin-esterase protein (HE protein) can also be found. S protein is a baseball-shaped glycoprotein protruding out of the envelope, which plays a key role in the binding of virus to the surface receptor of the host cells and in mediating membrane fusion into the host cells. It is also the main antigen protein of coronavirus. M protein is a transmembrane protein, which plays an important role in the formation of the virus envelope and budding. E protein is a relatively small protein mainly scattering at the virus envelope. The categorization of coronavirus and its structural pattern are illustrated in Figs. 20.1 and 20.2.

The resistance and stability of SARS-CoV in the external environment are stronger than other human coronaviruses. It can survive for 4 days on the dry plastic surface, at least 1 day in urine, over 4 days in stool of patients with diarrhea, and 15 days in the blood. On the surfaces of plastic, glass, mosaic, metal, cloth, and photocopy paper, it can survive for 2–3 days. SARS-CoV is sensitive to temperature, with weaker resistance at higher temperature. It can be inactivated at a temperature of 56 °C for 90 min and 75 °C for 30 min. SARS-CoV can be killed by diethyl ether at 4 °C for 24 h. And it can be inactivated by 75 % ethanol for 5 min or by disinfectants containing chlorine for 5 min. In addition, the virus is sensitive to ultraviolet radiation.

20.2 Epidemiology

20.2.1 Source of Infection

The patients are the major source of infection. At the acute stage, the patients carry a large quantity of viruses with serious respiratory symptoms, and the viruses are likely to be excreted from the respiratory tract. The patients with respiratory failure, especially those receiving tracheal cannulation or mechanical ventilation, have more secretions at the

L. Liang
Beijing You'an Hospital, Capital Medical University, Beijing, China
e-mail: Llc671215@sohu.com

H. Li (ed.), *Radiology of Infectious Diseases: Volume 1*, DOI 10.1007/978-94-017-9882-2_20

respiratory tract, with strong infectivity. The patients at the incubation period show low or no infectivity. The patients at the convalescent stage have not been reported to infect others. Epidemiological data have demonstrated that SARS-CoV mainly induces asymptomatic infection. Subclinical infection has not been sufficiently proved, and chronic patients carrying the virus have not been found.

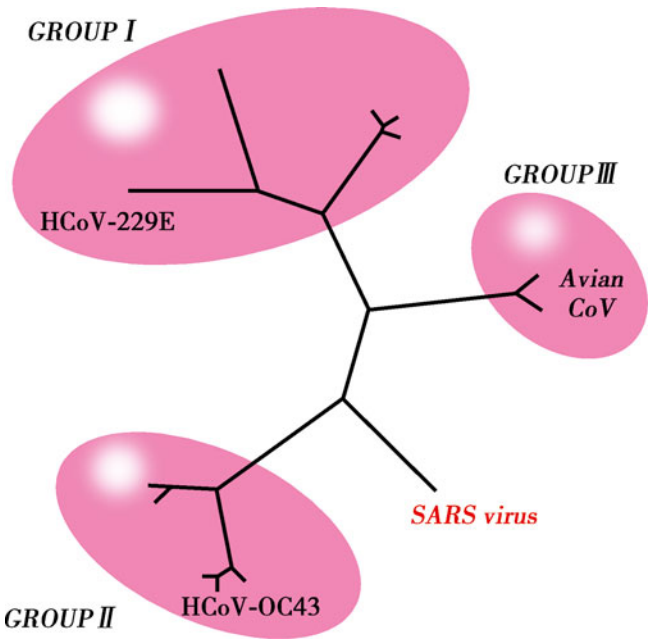

Fig. 20.1 Categorization of SARS coronavirus

Studies have demonstrated that the gene sequence of coronavirus isolated from civet cats and other animals is highly homologous with SARS-CoV, indicating that these animals may be the reservoir hosts of SARS-CoV and source of its infection. Therefore, SARS is likely to be an animal-borne infectious disease.

20.2.2 Route of Transmission

Spread by air droplets within a short distance is the major route of its transmission. In the throat swab and sputum specimen from patients at the acute stage, SARS-CoV can be detected. Spread along with aerosol is another route of its transmission. The susceptible individuals can be infected after inhalation of SARS-CoV containing aerosol suspended in the air. Spread via touches is also an important route of its transmission. For instance, the hands of susceptible individuals directly or indirectly touch secretions and excreta from the patients or utensils contaminated by the virus. Then the virus infects the human body via the mouth, nose, and ocular mucosa. Moreover, it can also be transmitted via virus-containing aerosol in the laboratory with inappropriately preserved SARS-CoV strains. In April 2004, a typical accident was reported that inappropriately preserved SARS-CoV strains in a laboratory in Beijing, China, caused five cases of infection with one case of death. During the epidemic period, nosocomial infection is more likely to occur. The main routes include: (1) Medical staff is infected by direct contact to the

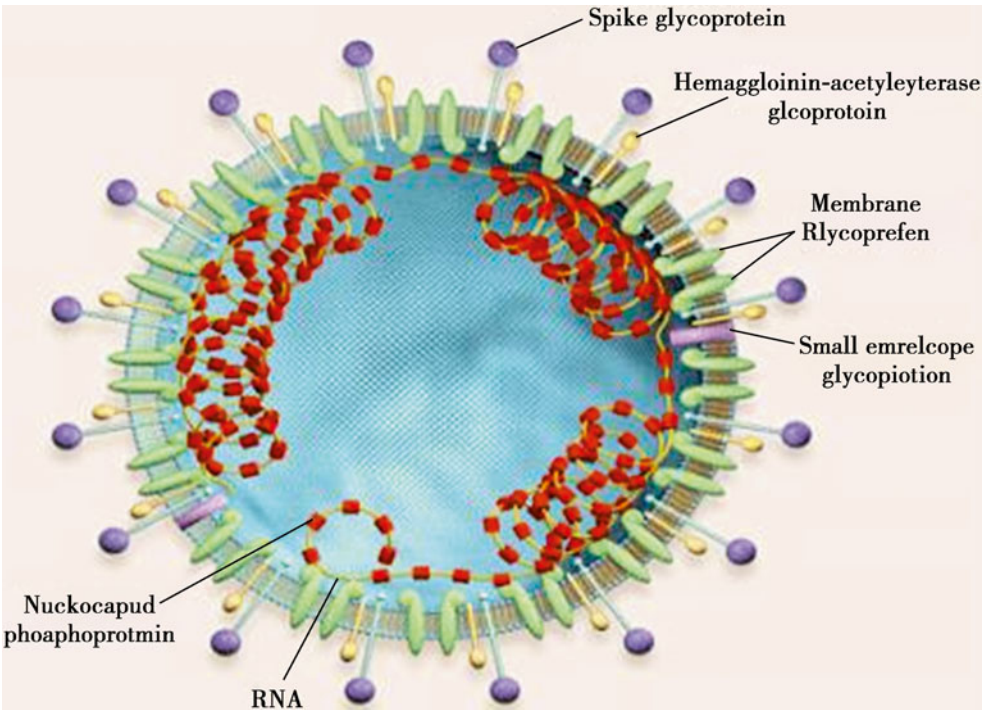

Fig. 20.2 Structural pattern of coronavirus particle

patients during treatment and attendance. The direct contacts are more likely to occur during oral cavity examination and tracheal cannulation with the medical staff inappropriately protected. (2) The visitors and those responsible for attending the patients are likely to be infected. (3) The patients with other diseases can be infected due to sharing the ward with a patient with SARS. Nosocomial infection is closely related to facilities of the ward, severity of the symptoms, stage the conditions are in, immunity of individuals with contact history, and personal protective measure of medical staff and visitor.

20.2.3 Susceptible Population

People are generally susceptible to SARS, with higher incidence in young adults and teenagers. But children and the elderly are also vulnerable to infection. The high-risk groups include family members of the patients, medical staff, nursing workers, and visitors. Based on data from You'an Hospital, Beijing, in 108 cases with clinically defined diagnosis of SARS, 31 cases are medical staff, accounting for 28.7 %; 32 cases are family members, 29.6 %. Cases of SARS complicated by diabetes, heart diseases, or other chronic diseases have higher mortality rate. After infection, the individuals can acquire certain immunity but its duration still needs further studies.

20.2.4 Epidemiological Features

20.2.4.1 Prevailing Seasons

SARS is a serious infectious disease with its earliest occurrence in the twenty-first century. It prevails in winters and springs, with occurrence of obvious familial and hospital agglomeration. Its occurrence in the community is mainly sporadic, with occasional occurrence of spot outbreak.

20.2.4.2 Chronological Distribution

In Nov. 2002, occurrence of SARS within members of one family was firstly reported in Foshan, Guangdong, China. In the following months, its occurrence rapidly spreads to more than 30 countries and regions including Guangzhou, Beijing, Hong Kong, Vietnam, and California. According to a report by the WHO, by June 20, 2003, prevalence of SARS had involved 28 countries and 32 regions across the world. A total of 8,461 cases had been reported, with 7,218 cases discharged from the hospital after treatment and 916 cases of death. The world average mortality rate of SARS is 9.5 %. In China, a total of 5,327 cases had been reported, with 4,959 cases cured and 349 cases of death.

20.2.4.3 Regional Distribution

Southeast Asia is the main affected area, especially mainland China, Hong Kong of China, Taiwan of China, Singapore, and Hanoi of Vietnam, followed by Thailand and the Philippines. Concerning Europe and America, the seriously affected area is Toronto in Canada, followed by the United States of America.

20.2.4.4 Age Distribution

Any age group may be affected, but mainly young and middle-aged adults (patients aged 20–49 years account for about 80 %). Its incidence rate has no gender difference. In cases of death, the elderly accounted for a larger proportion (about 40 % above the age of 60 years). And the mortality rate is higher in patients with SARS complicated by diabetes, heart diseases, or other chronic diseases.

20.3 Pathogenesis and Pathological Change

SARS-CoV is pantropic to human tissues, but its pathogenesis still remains elusive. It gains its access into the human body via the respiratory tract and replicates at the epithelium of respiratory mucosa. Then they are released into blood flow to cause viremia, with following invasion into various organs and tissues. And the virus mainly invades the lungs and immune system, with type I alveolar epithelial cells and lymphocytes possibly as its target cells.

By immunological assays, the specific antibody against SARS-CoV is detected in the serum, while SARS-CoV expresses M protein, N protein, S protein, and E protein to play its important pathogenic role. Clinically, SARS is characterized by acute lung inflammation and acute lung injury, with 5–10 % of cases complicated by ARDS and MODS. And the conditions of 90 % of such patients are self-limited. Lung inflammation caused by T lymphocytes is clinically parallel to its prognosis. By autopsy, pulmonary interstitial exudation, transudative inflammation, and alveolar injury are found. The germinal center of a lymph node is absent, and the count of lymphocytes decreases. Systemic inflammatory response syndrome (SIRS) involves the alveolar epithelial cells and pulmonary vascular endothelial cells to cause inflammatory congestion, further inducing large quantities of exudates of serous fluid and fibrinogen. The exudated fibrinogen agglutinates into cellulose, together with necrotic alveolar epithelial debris, to form hyaline membrane. The activated macrophages and lymphocytes can release cytokines and free radicals, which further increase the permeability of alveolar capillaries and induce the proliferation of fibroblasts. During the interaction of viruses with immune cells that infiltrate into the lung tissues, the host immune

cells (including macrophages, neutrophils, etc.) overproduce free radical molecules, such as oxygen radicals (O^{-}_{2}), nitric oxide radicals (NO), and its derivatives (ROS). Thus the infected cells and tissues are damaged.

The prominent pathological changes in cases of SARS occur at the lungs. Early pathological changes are characterized by pulmonary edema and formation of hyaline membrane. The advanced pathological changes include alveolar injuries, cellular and fibrous exudates, and interstitial infiltration of inflammatory cells with insufficient lymphocytes. By microscopic observation, the lungs are subject to diffuse exudative and acute hemorrhagic inflammation. There are also diffuse lesions of alveolar epithelial cells, highly dilated and congested alveolar capillaries, and apparent proliferation of alveolar wall due to edema and infiltration of lymphocytes and monocytes. Within most alveolar cavities, cellulose, erythrocytes, macrophages, and epithelial cells are observed, sometimes with formation of hyaline membrane. At the advanced stage, interstitial fibrosis and occlusion of alveolar fiber can be observed, with absent germinal center of a lymph node and decreased lymphocytes. Other organs, including the heart, liver, spleen, kidney, pancreas, and adrenal gland, are subject to different degrees of cellular hydropic degeneration, fatty degeneration, proliferation of interstitial cells, and other nonspecific pathological changes.

By autopsy of the death cases from SARS, it is demonstrated that SARS mainly involves the lungs and immune organs, such as the spleen and lymph node. Other organs, such as the heart, liver, kidney, adrenal glands, and brain, may also be involved with different degrees of lesions.

20.3.1 Lung

Generally, the lung in patients with SARS is apparently swollen, with increased weight. Except for cases with secondary infection, the pleura is quite smooth with a dark reddish or grayish brown color and with/without small quantity pleural effusion. On a section of lung tissue, homogeneous consolidation is commonly observed in a reddish brown or dark purplish color, which may involve any lung lobe resembling the hepatization stage of lobar pneumonia. In cases with secondary infection, abscesses in different sizes may be observed. The pulmonary vascular vessels are subject to thrombus and sometimes local pulmonary infarction (Fig. 20.3). In some cases, hilar lymphadenectasis can also be observed.

Under a light microscope, the pathological changes at the lungs are usually diffuse and almost involve all lung lobes. The changes are characterized by diffuse alveolar injury, with manifestations at different stages. At around day 10 of the illness course, the pathological changes include pulmonary edema, cellulose exudation, formation of hyaline membrane, desquamative pneumonia induced by accumulation of macrophages and shedding of type II alveolar epithelial cells

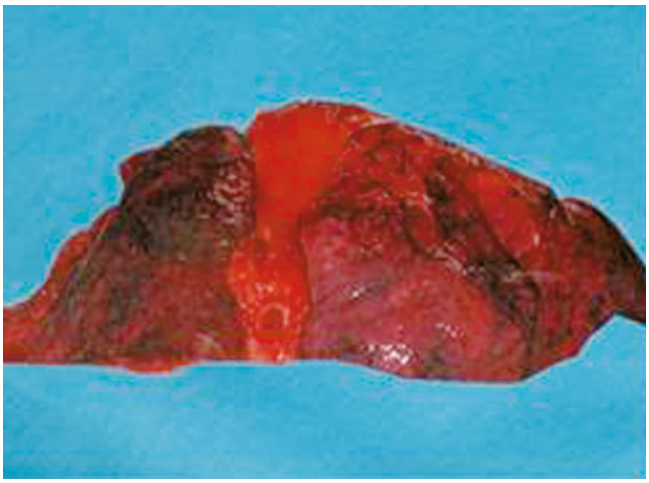

Fig. 20.3 Lung of SARS. By naked eyes observation, the lung is swollen with a dark reddish color and with hemorrhage lesions

in alveolar cavity, and focal pulmonary hemorrhage. These pathological changes can be observed on autopsy specimen and biopsy specimen collected by bronchofiberscopy. Some proliferated alveolar epithelium fuses into each other to form zygote-like multinucleated giant cells. In the proliferated alveolar epithelium and the cytoplasm of exudated monocyte, viral inclusion bodies can be observed (Fig. 20.4). Along with progress of the condition, in cases with an illness course exceeding 3 weeks, organization of intra-alveolar exudates and hyaline membrane as well as hyperplasia of fibroblasts in alveolar septum can be observed. Both of them constantly integrate to cause alveolar occlusion and atrophy, with consequent lung consolidation. Only in some cases, apparent fiber hyperplasia occurs to induce pulmonary fibrosis or even sclerosis. In intrapulmonary small blood vessels, fibroid microthrombus can often be found. For the above pathological changes, great individual difference can be found. Even in the lungs of one patient, pathological changes of different stages can be found. In some cases, especially those who have received long-term treatment, sporadic lobular pneumonia or even large-area fungal infection can be commonly found, and the most commonly found fungal infection is aspergillus infection. The secondary infections can involve the pleura to cause pleural effusion, pleural adhesion, or even occlusion of pleural cavity.

By electron microscopy, the alveolar epithelium is swollen, with apparent vacuolar degeneration of the mitochondria and endoplasmic reticulum. The alveolar epithelial cells are subject to proliferation, especially type II epithelial cells. For proliferated type II epithelial cells, the laminated body in the cytoplasm is decreased, with massive proliferation and expansion of both rough and smooth endoplasmic reticula. In the expanded endoplasmic reticulum cistern, protein secretions with increased electronic density are observed. In some expanded endoplasmic reticulum, clustering virus particles in uniform size can be observed, with tiny corolla-shaped

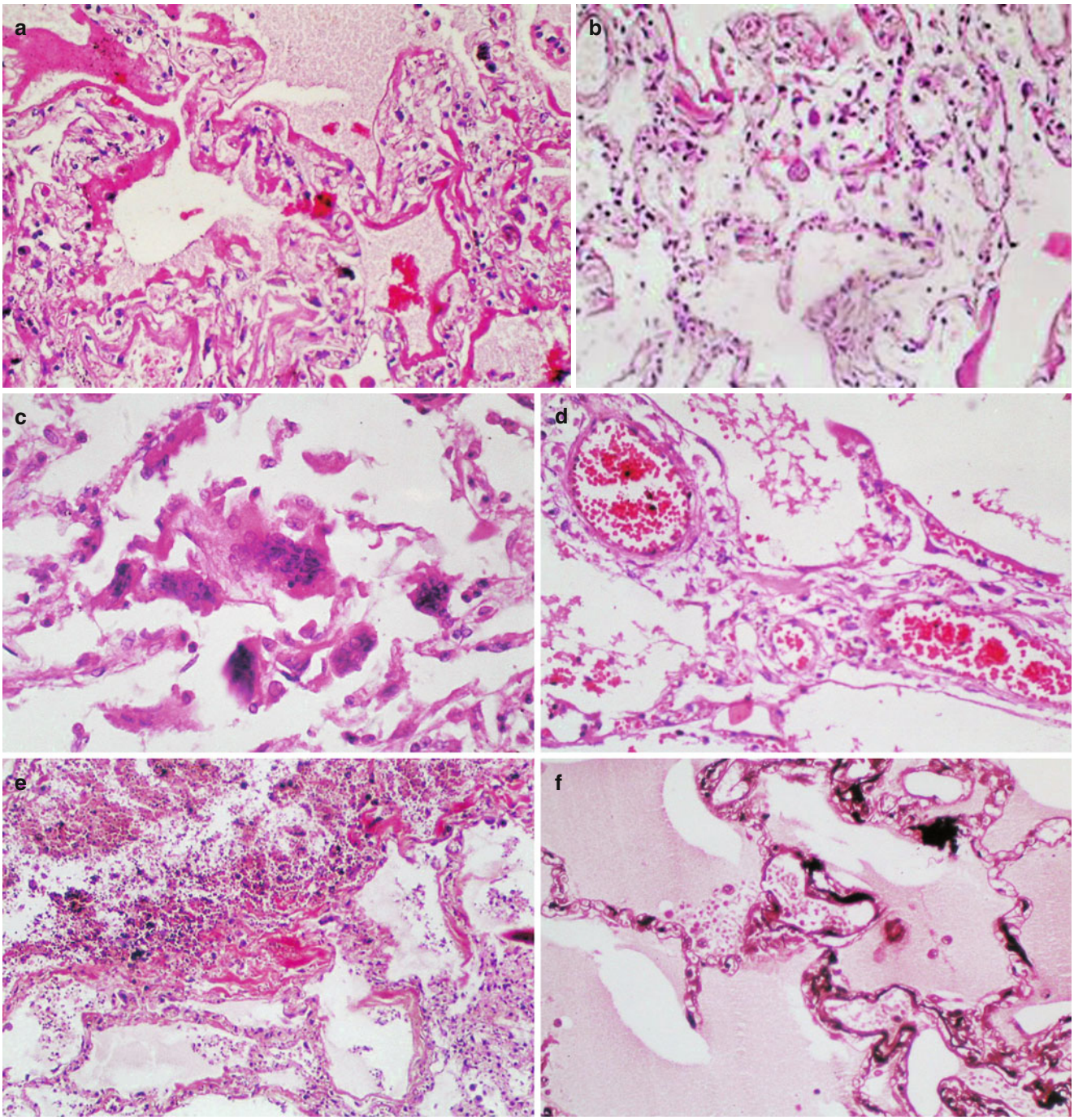

Fig. 20.4 Pulmonary pathological changes of SARS. (**a**) Evenly light-stained acidophilic exudates at the margin of alveolar cavity and formation of hyaline membrane (H&E, ×200). (**b**) Degeneration and necrosis of epithelial cells at the alveolar wall; shedding type II alveolar epithelial cells in the alveolar cavity; infiltration of small quantity lymphocytes and monocytes in alveolar septum (H&E, ×200). (**c**) Multinucleated giant cells in the alveolar cavity (H&E, ×400). (**d**) Obvious widening and edema of alveolar septum; dilation and congestion of interstitial blood vessels (H&E, ×400). (**e**) Hyperplasia of collagen fibers in alveolar septum, with a rose-red color and irregular shape (PTAH, ×200). (**f**) Hyperplasia of reticular fiber at alveolar capillary wall and the consequent irregular thickening of the capillary wall (reticular fiber, ×200). (**g**) Eosinophilic structure similar to virus inclusion body in alveolar epithelial cells, spherical in shape and surrounded with transparent halo sign (H&E, ×400). (**h**) Positively expressed N protein of SARS-CoV in cytoplasm of type II alveolar epithelial cells in the alveolar cavity, with red staining by AEC (immunohistochemistry, ×200). (**i**) Strong expression of NF-KB in cytoplasm of shed alveolar epithelial cells (immunohistochemistry, ×200). (**j**) In situ PCR demonstrates alveolar tissue with expressed nucleic acid of SARS-CoV in cytoplasm of alveolar epithelial cells, in blue-violet color (in situ PCR, ×400). (**k**) Positive expression of some c-kit in proliferated alveolar epithelial cells, with red staining by AEC (*arrow*) (immunohistochemistry, ×200). (**l**) Strong expression of TGF-β, in brownish-yellow color (immunohistochemistry, ×200). (**m**) Immunohistochemistry double-label staining demonstrates double positive, CD68 (*blue*) and NF-KB (*red*), of the shed cells in the alveolar cavity (immunohistochemistry, ×200). (**n**) Congestion and necrosis of hilar lymph nodes, decreased quantity of proper lymphocytes, and atrophy and absence of lymphatic nodules (H&E, ×400)

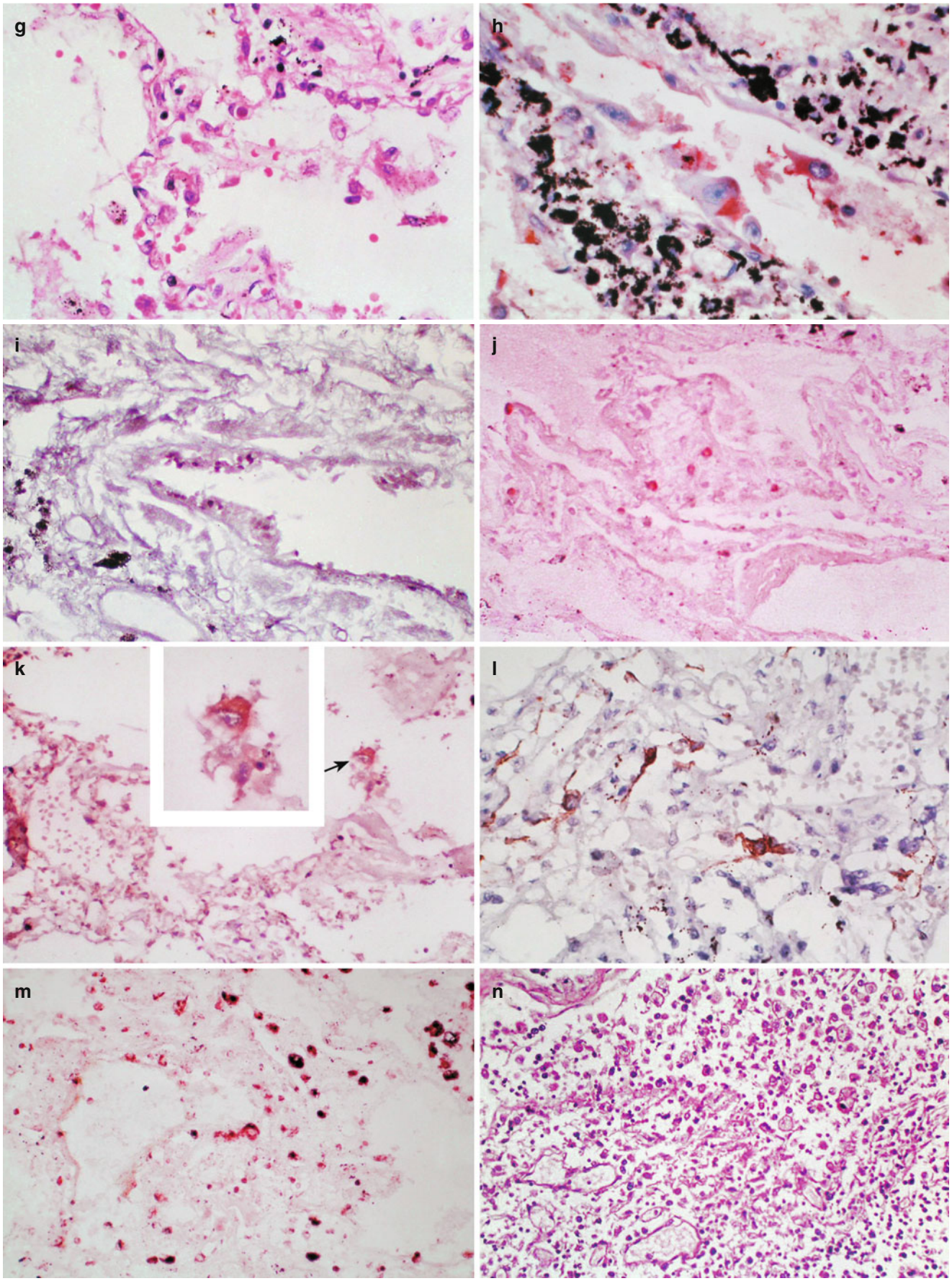

Fig. 20.4 (continued)

particles at their surface whose size is 60–120 nm. The interstitial vascular endothelial cells are subject to swelling and vacuolar degeneration.

20.3.2 Immune Organs

20.3.2.1 Spleen

In some patients with SARS, the spleen is subject to swelling but some shrinkage. On the spleen section of some cases, spleen mud can be observed. By microscopy, the spleen is subject to poorly defined splenic corpuscle, atrophy of white pulp, sparse lymphocytes with decreased quantity, congestion of red marrow, obvious bleeding and necrosis (Fig. 20.5), and increased histiocytes.

20.3.2.2 Lymph Node (Abdominal Lymph Nodes and Hilar Lymph Nodes)

In some cases, swelling of the lymph nodes can be observed. Microscopy has demonstrated that almost all lymph nodes are subject to atrophy and absence of lymph follicles but with different degrees. The lymphocytes are sparsely distributed, with decreased quantity. The vascular vessels and lymph sinus are subject to obvious dilation and congestion, with obvious proliferation of sinus histiocytes and even bleeding and necrosis in some cases.

20.3.3 Pathological Changes of Other Organs

20.3.3.1 Liver

In most cases, the hepatocytes are subject to slight hydropic degeneration, focal fatty degeneration, and cord dissociation. In the liver lobule, the Kupffer cells are obviously increased, with infiltration of small quantity lymphocytes at the portal area (Fig. 20.6). In some cases, obvious hepatocytic necrosis can be found around the central vein.

20.3.3.2 Heart

In patients with SARS, cardiac hypertrophy is common, generally characterized by uniform thickening of the left and right heart. Interstitial edema of the myocardium is obvious,

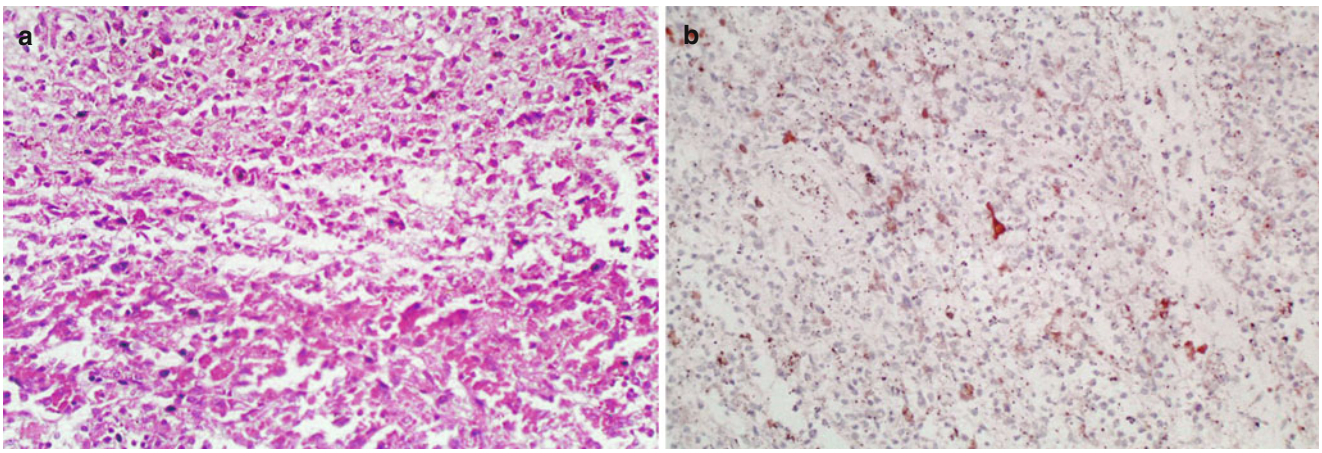

Fig. 20.5 Splenic pathological changes of SARS. (**a**) Focal hemorrhage and necrosis in the spleen and atrophy of the white pulp (H&E, ×200). (**b**) S-100-positive lymphocytes in the spleen (immunohistochemistry, ×200)

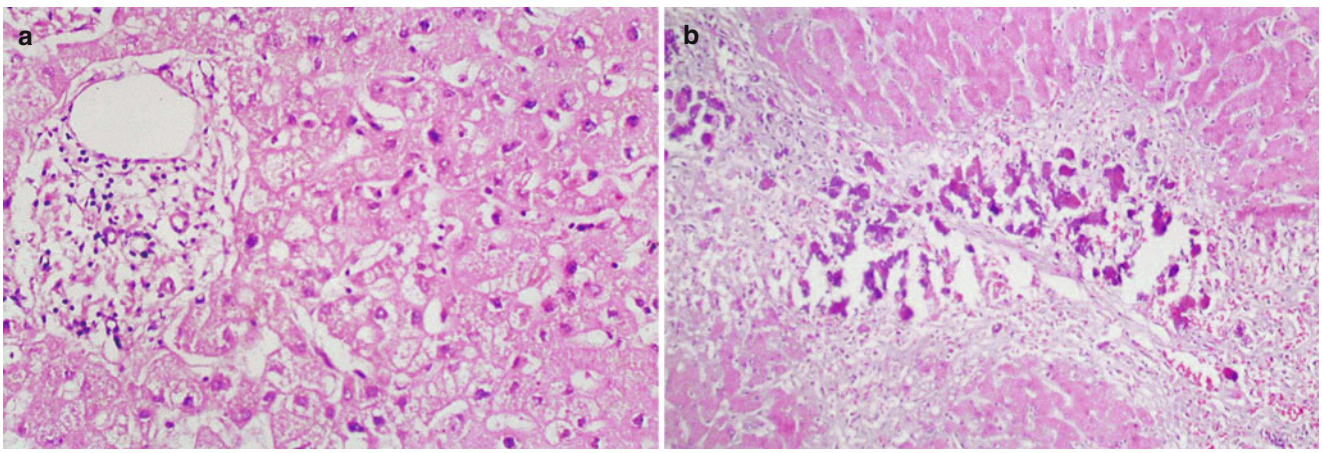

Fig. 20.6 Hepatic pathological changes of SARS. (**a**) Swollen hepatocytes, proliferation of intralobular Kupffer cells, slightly enlarged portal area, and infiltration of small quantity monocytes (H&E, ×400). (**b**) Flakes and strips of necrosis of hepatocytes at lobular area III (H&E, ×400)

with interstitial infiltration of sporadic lymphocytes and monocytes. In some cases, the myocardial cells are subject to vacuolar degeneration, focal myocarditis, and small focal necrosis. Severe secondary infection, such as fungal infection, can also involve the heart (Fig. 20.7).

20.3.3.3 Kidney

In most patients with SARS, obvious glomerular congestion and degeneration of epithelial cells at the renal tubules can be found. In some cases, extensive fibrinous thrombus in glomerular capillaries can be found. In some cases, there are intramedullary small focal necrosis and infiltration of lymphocytes and monocytes. Dilation and congestion of renal interstitial vascular vessels are also found. In some cases, small pyogenic lesions can be found due to secondary infection, with occasional occurrence of vasculitis.

20.3.3.4 Adrenal Glands

In some cases, focal hemorrhage can be found at the cortex and medulla, with necrosis, infiltration of lymphocytes, vacuolar degeneration of cortical fascicular cells, and/or decreased content of adipoid tissue.

20.3.3.5 Brain

The brain tissue is subject to varying degrees of edema and sometimes sporadic neuronal ischemic changes. In severe cases, the brain tissue is even subject to necrosis. Some nerve fibers are subject to demyelization.

20.3.3.6 Bone Marrow

In most patients, the counts of neutrophils and the megakaryocytic system in hemopoietic tissue are subject to relative decrease. In some cases, erythroid cells are characterized by small focalized proliferation.

20.3.3.7 Gastrointestinal Tract

The submucosal lymphatic tissue is decreased at each segment of the stomach, small intestine, and colon, with sparse lymphocytes and interstitial edema. In some cases, superficial erosion or ulceration can be found at the stomach.

20.3.3.8 Pancreas

Interstitial vascular congestion is found. In some cases, slight interstitial fibrous proliferation and infiltration of lymphocytes can be found. There are also acinar atrophy at exocrine glands, decreased zymogen granules, and degeneration of some islet cells (Fig. 20.8).

The gallbladder is demonstrated with no obvious pathological changes.

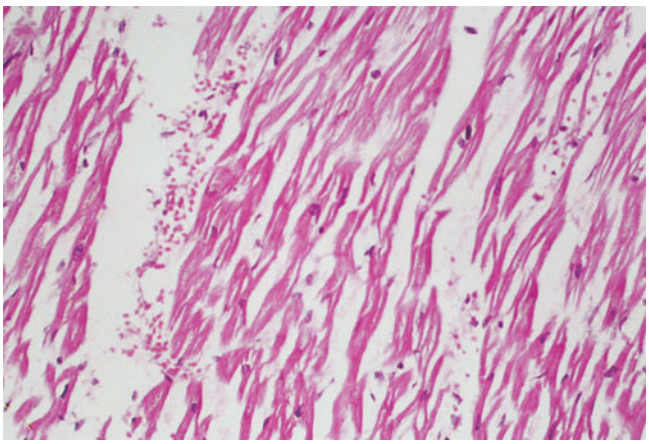

Fig. 20.7 Cardiac pathological changes of SARS. Atrophy of myocardial cells, congestion and edema between cells, and infiltration of small quantity monocytes (H&E, ×200)

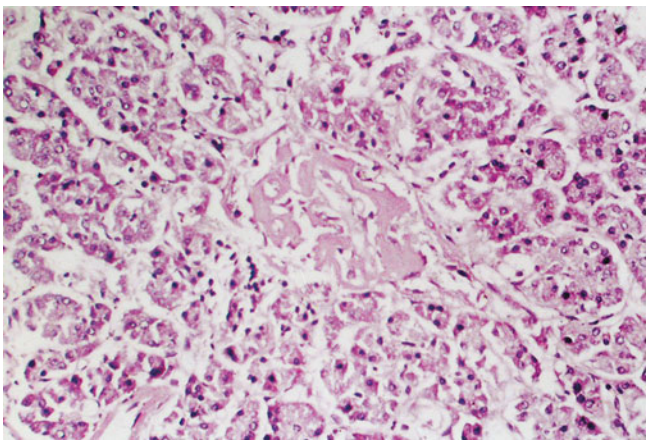

Fig. 20.8 Pancreatic pathological changes of SARS. Atrophy of pancreatic acinus, infiltration of a small quantity of monocytes in interstitial tissue, and hyaline degeneration of islet (H&E, ×200)

20.3.3.9 Reproductive System

The testis is sometimes subject to degeneration of spermatogenic cells, with reduced spermatogenesis. Interstitial vascular dilation and hemorrhage can be observed.

The prostate, uterus, ovaries, and fallopian tubes are demonstrated with no obvious pathological changes.

In addition, polyangiitis based on venules can be found at the lungs, heart, liver, kidney, brain, adrenal glands, and striated muscle of some cases. Polyangiitis is characterized by edema of vascular wall and perivascular tissue, swelling and apoptosis of vascular endothelial cells, fibrinoid necrosis of vascular wall, and infiltration of monocytes and lymphocytes at vascular wall and perivascular tissue.

20.4 Clinical Symptoms and Signs

The incubation period lasts generally for 1–16 days, averagely 3–5 days. In extremely rare cases, it may last for as long as 20 days.

20.4.1 Main Symptoms

20.4.1.1 Fever

Fever is the initial symptom at onset, mostly high fever that is remittent or irregular and occasional accompanying chills.

20.4.1.2 Systemic Toxic Symptoms

The patients experience systemic toxic symptoms, such as headache, joint soreness, general soreness, fatigue, chest pain, and diarrhea.

20.4.1.3 Respiratory Symptoms

Cough possibly occurs that is mostly dry cough at the early stage, with rare sputum and chest distress. The patients experience no upper respiratory catarrhal symptoms. Along with progress of the conditions, the symptoms aggravate, with shortness of breath and frequent irritated cough with whitish thick or bloody sputum. In cases complicated by bacterial or fungal infection, sputum may be yellowish or foamy. In severe cases, the patients also experience asthmatic suffocation and dyspnea, which may further develop into acute respiratory distress syndrome.

20.4.1.4 Pulmonary Signs

The pulmonary signs are commonly not obvious. Some patients may show dry and/or moist rales at the lungs or lung consolidation sign. Occasionally, signs of small quantity pleural effusion may be found, with local dull sound by percussion and decreased breathing sound.

20.4.2 Clinical Staging

According to the clinical guideline for SARS stipulated by the Chinese Medical Association and Chinese Traditional Medicine Society on Sept. 30, 2003, SARS is clinically staged into the early stage, the progressive stage, and the convalescent stage.

20.4.2.1 The Early Stage

Generally, the early stage refers to the initial 1–7 days after the onset. The disease had an acute onset with fever as its initial symptom. The body temperature is commonly above 38 °C, and more than half of patients experience headache, joint and muscle soreness, fatigue, and other symptoms. Some patients may also experience dry cough, chest pain, and diarrhea but rarely experience upper respiratory catarrhal symptoms, mostly with no obvious lung signs. In some patients, rare moist rales can be heard at the lungs. X-rays demonstrate the appearance of lung shadows at day 2 after the onset, averagely 4 days. Over 95 % of the patients are demonstrated with positive lesions at day 7 after the onset.

20.4.2.2 The Progressive Stage

The progressive stage refers to days 8–14 after the onset, but even longer for individual cases. During this stage, fever and toxic symptoms persist, with progress of lung lesions. Clinically, it is characterized by chest distress, shortness of breath, dyspnea, and tachycardia, which are especially obvious after physical activities. X-rays demonstrate rapid progress of lung shadows, which commonly involve multiple lung lobes. Rare patients (about 10–15 %) develop life-threatening ARDS.

20.4.2.3 The Convalescent Stage

After the progressive stage, the body temperature begins to decrease gradually, with alleviated clinical symptoms and absorbed lung lesions. Most patients are healed within about 2 weeks and can be discharged from the hospital. The absorption of lung lesions needs more time. In rare severe cases, restrictive ventilation disturbance and diffusion dysfunction of lungs may remain for a longer period of time, mostly returning to normal within 2–3 months after discharge.

20.5 SARS-Related Complications

Typical SARS undergoes three main stages: virus replication, abnormally active immune system, and organ damage. During the development of SARS and the therapeutic intervention, the possible complications are listed as the following:

20.5.1 Secondary Infection

Critical and severe cases of SARS sustain serious organ damages; in addition to compromised immunity, tracheal cannulation, and various invasive procedures, the patients commonly experience secondary bacterial and fungal infections. The elderly, patients with underlying chronic disease, patients with long-term management in the ICU, and those using immunosuppressive agents are especially vulnerable to these complications. Experts in Beijing have analyzed clinical data of 190 death cases from SARS, and they found

that 46.3 % of cases underwent secondary infection of varying degrees, with 34 cases (36.8 %) of secondary bacterial infection, 32 cases (36.4 %) of secondary fungal infection, 2 cases of tuberculosis, and 20 cases (22.7 %) of secondary mixed infection. Accordingly, when rescuing patients with SARS, especially during use of large doses of hormones, the practitioners should be highly alert to the occurrence of secondary infections, with early precautions and active treatments.

20.5.2 ARDS and MODS

Most patients with SARS are basically healed after comprehensive treatment for 2–3 weeks. But some of the patients experience progressive aggravation of the conditions and develop acute respiratory distress syndrome (ARDS). Some patients even develop multiple organ dysfunction syndrome (MODS) and failure, with final occurrence of clinical death.

20.5.2.1 ARDS

The typical symptom of ARDS is respiratory distress, including varying degrees of cough, asthmatic suffocation, shortness of breath, and progressive dyspnea. The primary respiratory symptoms of SARS aggravate, and the patients develop typical bloody sputum at the advanced stage, with consciousness disturbances. By auscultation, bronchial breathing sounds, dry rales, crackles, or even bubbling sound can be heard at the lungs. Chest X-ray demonstrates infiltrative shadows at both lungs. The cases with a gas pressure at pulmonary capillary not higher than 18 mmHg or with clinically excluded cardiac pulmonary edema can be diagnosed as ARDS.

20.5.2.2 MODS

Organ damages, systemic inflammatory response syndrome, refractory hypoxemia, secondary infection due to combined use of large doses of hormones and diverse antibiotics, stress responses of the human body, and persistent high metabolism can induce severe types of cases that progress into MODS. Consequently, clinical death occurs. In addition to the lungs, the kidney, heart, liver, brain, and gastrointestinal tract are susceptible to severe damages caused by SARS viruses.

20.5.3 Pulmonary Interstitial Fibrosis

Pulmonary inflammation persists for a certain period of time. Along with tissue repair, proliferation of interstitial cells and formation of a large quantity of matrix occur, constituting the basis for pulmonary fibrosis. Pulmonary fibrosis is characterized by multiple cord-like and grid-like shadows at the lungs. Diffuse pulmonary parenchymal inflammation causes extensive lung lesions. Sustained progress of pulmonary fibrosis can finally lead to honeycomb lung and further induces localized secondary emphysema. The affected thorax is then subject to shrinkage. The clinical manifestations include progressive dyspnea and irritated dry cough. Although the pathomechanism of pulmonary fibrosis in cases of SARS has remained largely unknown, it is defined that persistent pulmonary inflammation may be an important factor contributing to the occurrence of pulmonary fibrosis in cases of SARS.

20.5.4 Mediastinal Emphysema, Subcutaneous Emphysema, and Pneumothorax

Pulmonary parenchymal inflammation, characterized by congestion, necrosis, and increased intrapulmonary pressure, causes alveolar rupture and consequent interstitial edema. The air flows along the major vascular vessels or bronchus to the hilum and finally reaches the mediastina as well as subcutaneous soft tissues. In some cases, mediastinal emphysema, subcutaneous emphysema, and pneumothorax occur after the use of respirator.

Intrapulmonary lesions can cause localized thickening of adjacent pleura or slight curtain-like adhesion. Pleural changes can be absent along with absorption of intrapulmonary lesions. Apparent pleural effusion is rarely found.

20.5.5 Bone Change

Due to severe anoxia, inappropriate use of hormones, and individual body constitution of patients with SARS, bone changes occur. The bone changes are more commonly found at the hip and knee joints and can also be found at the ankle, shoulder, and diaphysis of the long bone. The bone changes are characterized by osteoporosis and ischemic necrosis. The patients with ischemic necrosis of the femoral head experience hip pain that is occult, progressive, and dull as well as slight limp or intermittent limp. About one-third of the patients experience intermittent pain, with sudden severe pain and sudden absence of pain. During the attack of pain, the patients sustain joint dysfunction that can be immediately relieved after medication of hormones. At the early stage, examinations only demonstrate localized pressing pain and limited joint rotation. At the middle and advanced stages, the point of tenderness is commonly located at the middle point of the inguinal region, with obviously limited movement of the hip joint. The patients with the above symptoms at the advanced stage should immediately consult a specialist to receive X-ray, CT scanning, or MR imaging examination.

20.5.6 Digestive Complications

Some patients sustain varying degrees of digestive diseases at different stages of SARS. It has been reported in Beijing that 21.7–27.6 % of cases develop diarrhea (in Hong Kong 73 % reported by Peiris et al.), 11.5–15.8 % nausea and vomiting, 23.5–65.85 % liver dysfunction, and 13 % slight jaundice. The occurrence of these digestive symptoms is related to the severity of the conditions. Common types of symptoms the patients experience are transient digestive symptoms, which can be alleviated along with improved conditions or decreased dose of medication. Pathology demonstrated that the liver is subject to nonspecific inflammatory response. Autopsy and pathology based on 3 death cases have demonstrated that the hepatocytes are subject to slight swelling, fatty degeneration, proliferative and active liver sinus cells, slightly enlarged portal area, and infiltration of small quantity lymphocytes. These inflammatory responses correspond to the clinical manifestations.

20.5.7 Cardiovascular Complications

SARS virus may invade the myocardium to cause nonspecific inflammatory changes, such as myocardial interstitial edema, slight proliferation of interstitial cells, and infiltration of a small quantity of lymphocytes. Biochemistry demonstrates abnormal myocardial enzyme spectrum, which is mainly characterized by increases of lactate dehydrogenase, creatine kinase, and hydroxybutyrate dehydrogenase. Zhao JM et al. have found SARS virus particles in myocardial cells by autopsy of death cases from SARS. It is believed to be related to clinical findings of arrhythmia and abnormal myocardial enzyme spectrum. The patients experience different degrees of palpitation, chest distress, and arrhythmia. The most common ECG abnormality is sinus tachycardia, followed by ST-T dynamic change, sinus bradycardia, and atrioventricular block.

20.5.8 SARS-Related Psychiatric Disorders

The occurrence of SARS-related psychiatric disorders is dependent on the disease itself, personal psychological quality, and social factors. Due to the extremely high infectivity and pathogenicity as well as its consequent organ dysfunctions and quarantined environment for treatment, psychiatric disorders may occur in patients with SARS. The psychiatric disorders include panic, anxiety, depression, excitement, sleep disorders, or even delirium. Extremely rare patients even may commit suicide.

20.6 Diagnostic Examinations

20.6.1 Laboratory Test

20.6.1.1 Common Test

Routine Blood Test

At the early and middle stages of the disease, the WBC count is normal or decreased, and the absolute value of lymphocyte count drops.

Blood Biochemistry

Lactate dehydrogenase and aminotransferase in some patients increase in different degrees. By blood gas analysis, hypoxemia can be detected.

Serological Test

WTO recommended ELISA or IFA as the way to detect serum antibody against SARS-CoV. After day 11 of the illness course, the specific antibody against SARS-CoV significantly increases. By ELISA, its sensitivity and specificity to specific IgM antibody are respectively 70.16 % and 97.9 % and to specific IgG antibody are respectively 88.3 % and 99 %. By IFA, its sensitivity and specificity to specific IgM antibody are respectively 65.6 % and 100 % and to specific IgG antibody are respectively 91.1 % and 97 %. Both the tests facilitate to define the diagnosis for cases with an illness course of above 10 days.

Etiological Test

By RT-PCR, the finding of SARS-CoV RNA in the specimens of blood, airway secretions, urine, and feces has significance for early diagnosis. The examination has high specificity but poor sensitivity. Therefore, the negative finding cannot exclude the possibility of SARS.

20.6.2 Radiological Examination

20.6.2.1 Radiological Technology

Chest X-ray and CT scanning are the main examinations for the diagnosis of SARS. Standing posture is commonly adopted for posterior-anterior X-ray examination. If permitted, bedside chest X-ray should be performed at sitting posture for posterior-anterior examination. Digitized radiological examinations, such as computed radiography (CR) and digital radiography (DR), improve diagnostic accuracy of chest X-ray. CT scanning can detect lesions that fail to be detected by chest X-ray, and high-resolution CT (HRCT) is commonly recommended. Imaging examination procedures established on the basis of picture archiving and communication system (PACS) can improve examining efficiency and reduce cross infection.

Radiological practitioners should strictly observe the disinfection and protective procedures to prevent infection. Meanwhile, preventive measures from X-ray radiation should also be strictly implemented.

20.6.2.2 Radiological Procedures

Initial Examination

Chest X-ray is the examination of choice for patients who are clinically suspected with SARS. For the cases with no abnormality by chest X-ray, reexaminations should be performed. If possible, CT scanning should be ordered.

Follow-Up Examination During Treatment

During the treatment of SARS, chest X-ray examinations should be performed to assess the conditions and the therapeutic efficacy. Commonly reexamination by chest X-ray should be performed once every 1–3 days. The frequency of chest X-ray reexaminations can be modified based on the stage and therapeutic effect. For the cases with suspected cavity or fibrosis at the lungs by chest X-ray, CT scanning should be ordered.

Follow-Up Examination After Discharge from Hospital

After the patients are discharged from the hospital, X-ray examinations should be regularly performed until complete absorption of the inflammatory lesions.

20.7 Imaging Demonstrations

X-ray and CT scanning basically demonstrate ground-glass opacity and pulmonary consolidation.

20.7.1 The Early Stage

Radiological examination provides an important basis for early diagnosis of SARS. Based on a group of patients with SARS in You'an Hospital, Beijing, China, the clinical data indicated that all the patients have abnormalities by chest CT scanning, while the detection rate of chest X-ray is only 30 %. Chest X-ray demonstrates small flakes of blurry shadows with light density and with rare large flakes of blurry shadows. CT/HRCT demonstrates round-like or flakes of ground-glass opacities, dilated vascular shadow in some lesions, and surrounding thickened bronchovascular bundle. Most of the lesions are located at the lateral part of the lungs or under the pleura. The lesions are commonly demonstrated as the following:

20.7.1.1 Singular Small Flake of Shadow

Singular small flake of shadow is demonstrated in about 80 % of cases and is morphologically categorized into three types:

Round-Like Ground-Glass Opacity

The lesions are demonstrated as round-like ground-glass opacity with low density and poorly defined boundary in a size of 1–3 cm. In the shadows of the lesions, the vascular shadows are obviously thickened, with central consolidation in high density. The bronchovascular bundle adjacent to the lesions is demonstrated to be thickened (Fig. 20.9).

Pulmonary Lobular or Lobular Fusion-Like Ground-Glass Opacity

Chest X-ray demonstrates small flakes or one segmental blurry shadow. CT scanning shows well-defined lesions with a range of pulmonary lobule and lobular fusion, in shape of lobule or segment. The lesions are demonstrated with ground-glass density and surrounding thickening of interlobular septum of some lesions (Fig. 20.10).

Small Flakes of Consolidation

Chest X-ray demonstrates flakes of blurry shadows. CT scanning shows the lesions with high density and poorly defined boundary. The lesions are surrounded by ground-glass density lesions, with consolidation that displays air bronchus sign (Figs. 20.11, 20.12, 20.13, and 20.14).

Case Study 1

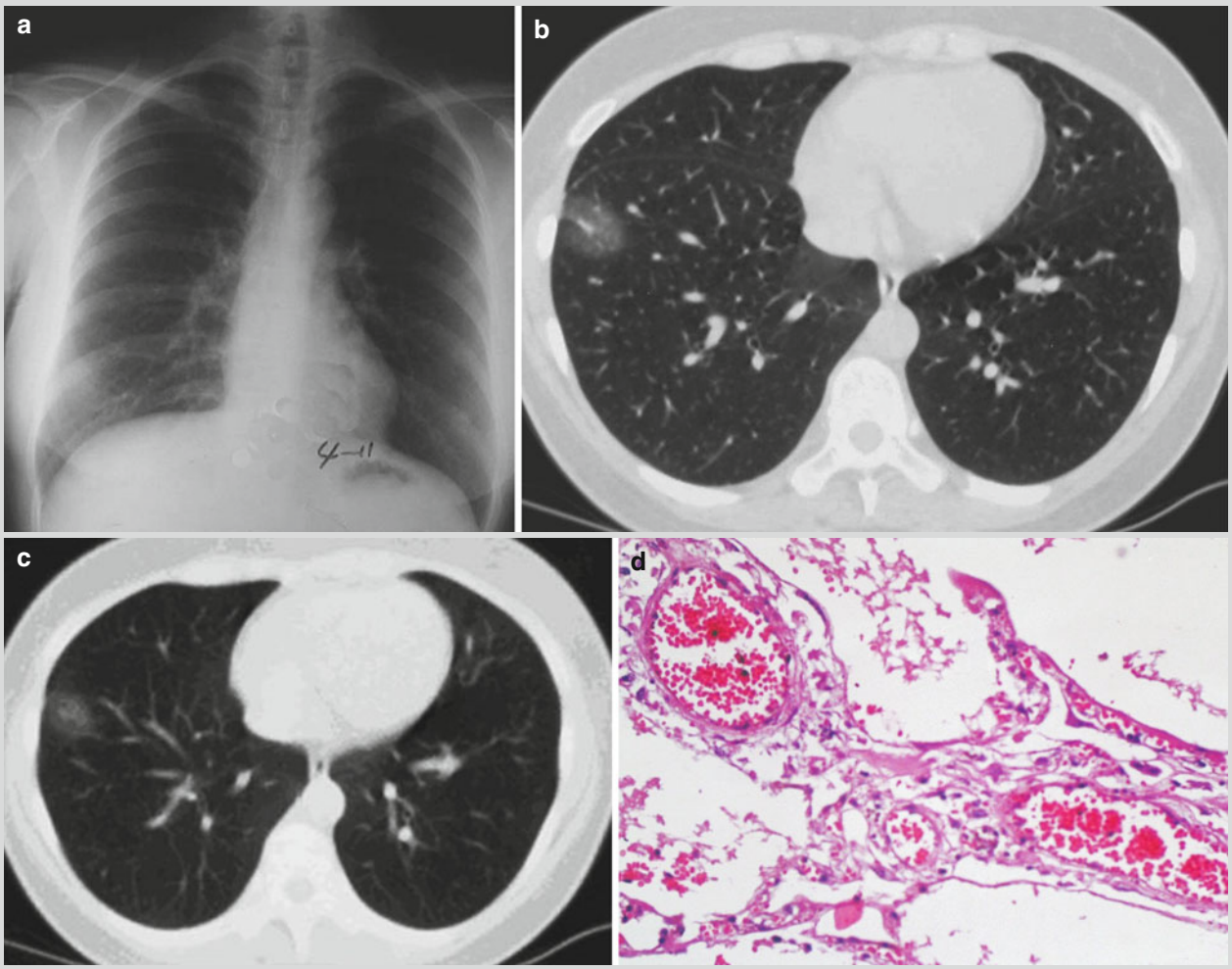

Fig. 20.9 SARS. (**a**) At day 1 of the illness course, chest X-ray demonstrates subpleural flakes of blurry shadow at the right lower lung. (**b**) CT scanning demonstrates ground-glass opacity at the right lower lung lobe. (**c**) HRCT demonstrates dilated vascular shadow in the lesions. (**d**) Pathology demonstrates obvious thickening and edema of the alveolar septum as well as dilation and congestion of interstitial vascular vessels (H&E, ×400)

Case Study 2

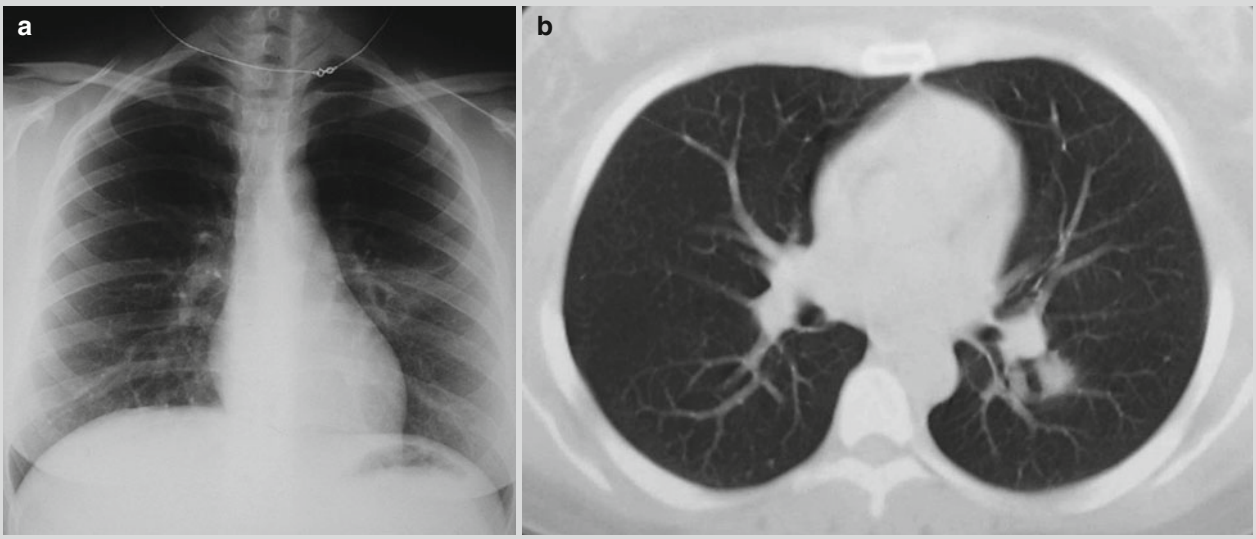

Fig. 20.10 SARS. (**a**) At day 2 of the illness course, chest X-ray demonstrates small flakes of shadow at the left hilum. (**b**) At day 1 of the illness course, CT scanning demonstrates small flakes of ground-glass opacity at the left lower lung lobe

Case Study 3

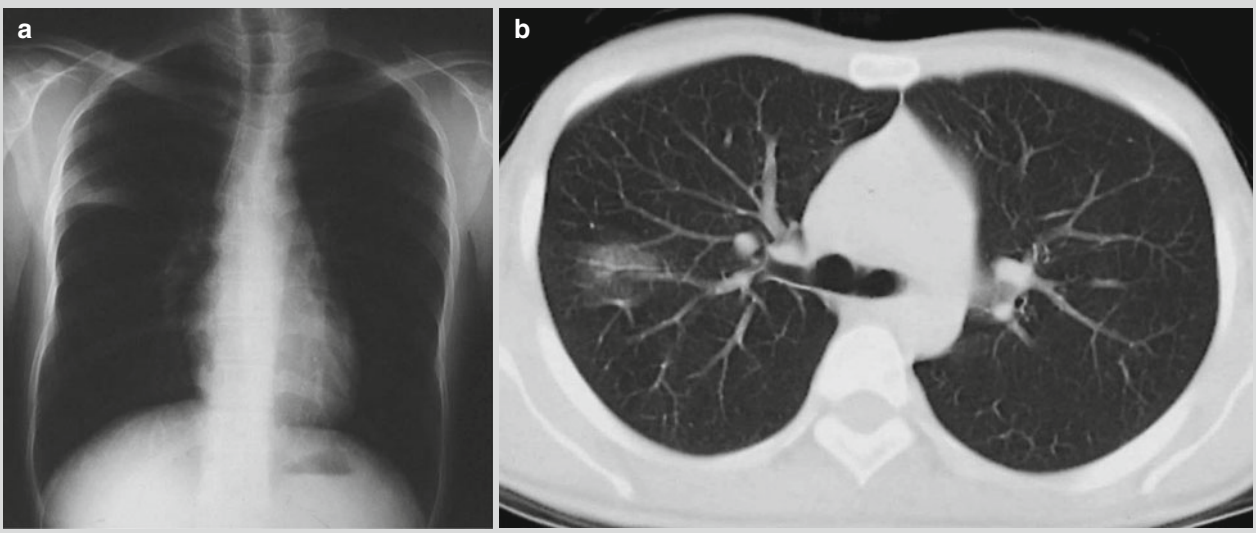

Fig. 20.11 SARS. (**a**) At day 1 of the illness course, chest X-ray demonstrates subpleural triangular blurry shadow at the right upper lung lobe. (**b**) CT scanning demonstrates ground-glass opacity at the left upper lung lobe

Case Study 4

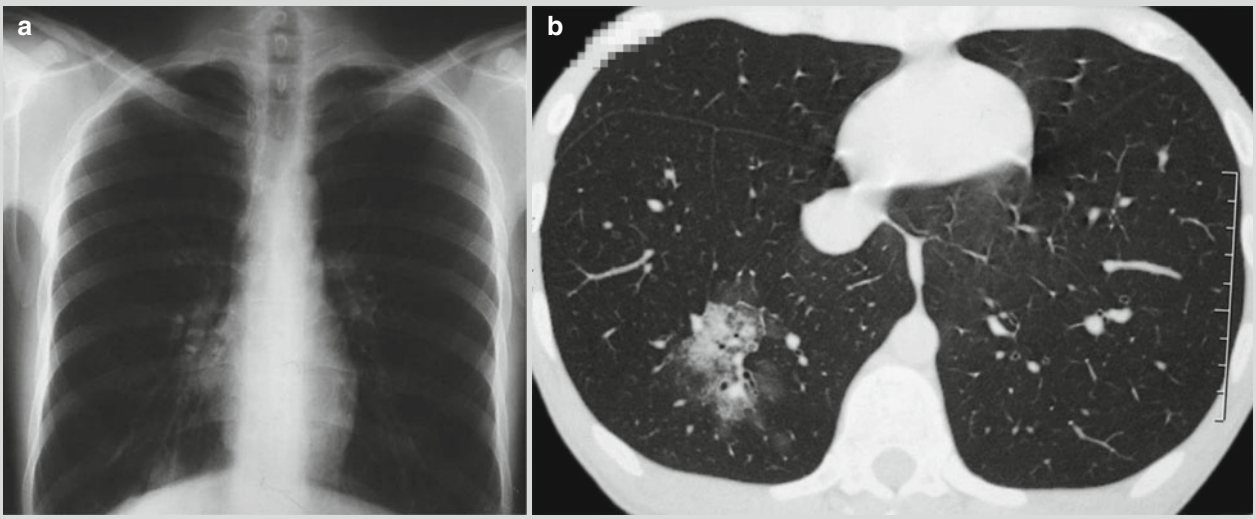

Fig. 20.12 SARS. (**a**) At day 3 of the illness course, chest X-ray demonstrates ground-glass opacity at the right lower lung lobe. (**b**) CT scanning demonstrates lobular fusion-like ground-glass opacity at the right lower lung lobe, with inner consolidation

Case Study 5

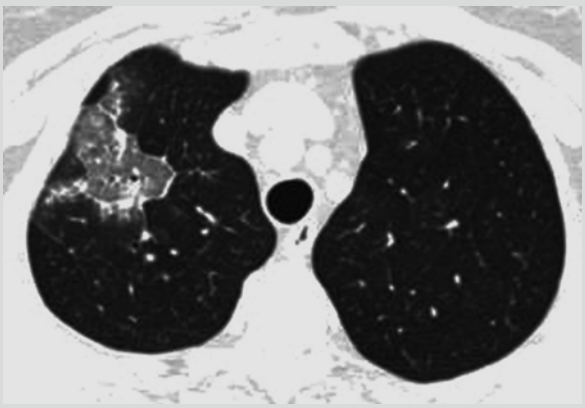

Fig. 20.13 SRAS. At day 3 of the illness course, CT scanning demonstrates lobular fusion-like ground-glass shadow at the right upper lung lobe

Case Study 6

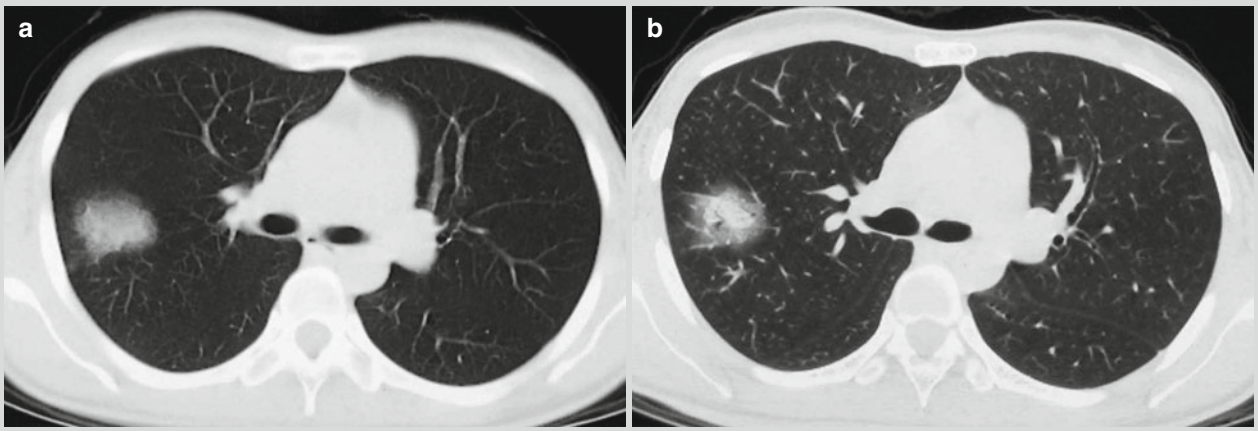

Fig. 20.14 SARS. (**a**) At day 4 of the illness course, CT scanning demonstrates patches of ground-glass shadow at the right upper lung lobe. (**b**) HRCT demonstrates patches of ground-glass shadow at the right upper lung lobe, with inner consolidation

20.7.1.2 Multiple Small Flakes of Ground-Glass Opacity

At both lungs, multiple round-like ground-glass opacities can be demonstrated (Figs. 20.15, 20.16, and 20.17). Chest X-ray demonstrates small flakes of blurry shadows. The smaller lesions are commonly failed to be demonstrated.

Case Study 7

Fig. 20.15 SARS. At day 3 of the illness course, CT scanning demonstrates multiple round-like ground-glass opacities at both lungs with different sizes

Case Study 8

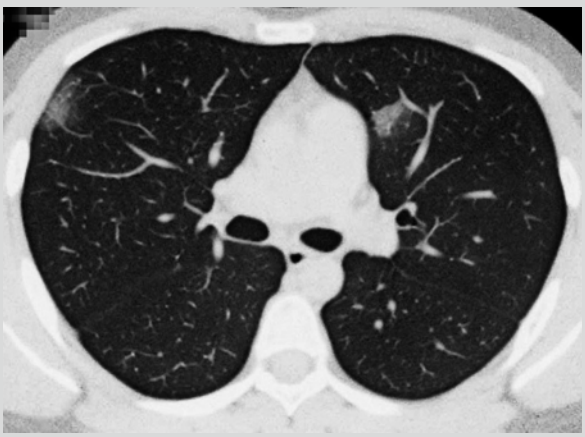

Fig. 20.16 SARS. At day 3 of the illness course, CT scanning demonstrates multiple flakes of ground-glass shadows at bilateral upper lung lobes

Case Study 9

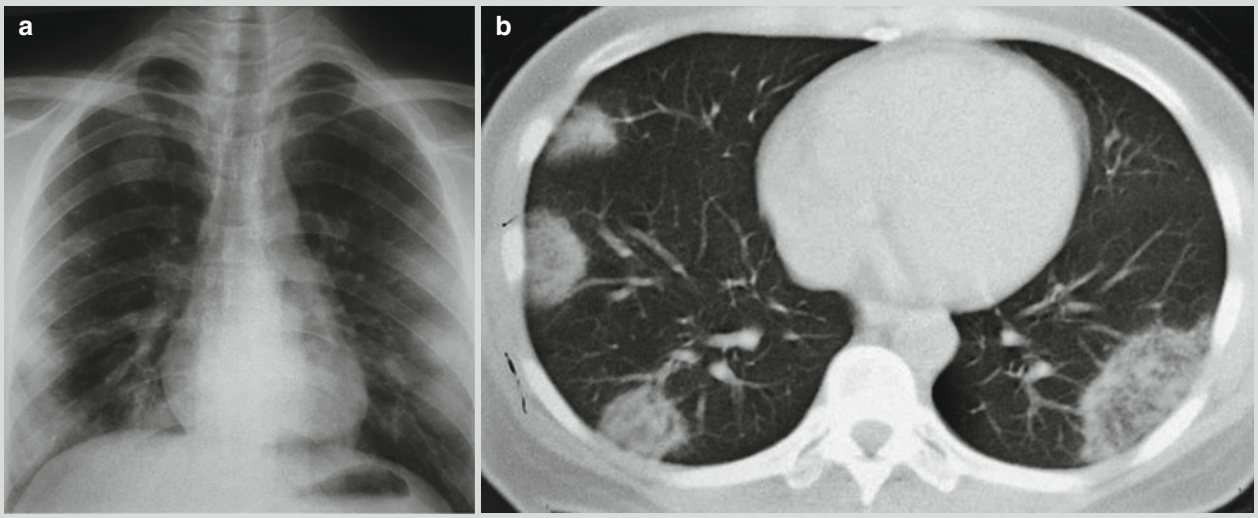

Fig. 20.17 SARS. (**a**) X-ray demonstrates subpleural beads string-like round-like ground-glass shadow at both lungs. (**b**) CT scanning demonstrates subpleural multiple ground-glass shadows at both lungs, with different shapes and uneven density

20.7.1.3 Large Flake of or Segmental Ground-Glass Opacity

Chest X-ray demonstrates flakes of blurry shadows, failed demonstration of the fused ground-glass opacities, and the range with lesions corresponding to segmental range (Figs. 20.18 and 20.19). CT scanning can clearly display the location of lesions (Figs. 20.20 and 20.21).

Case Study 10

Fig. 20.18 SARS. At day 3 of the illness course, chest X-ray demonstrates wedge-shaped ground-glass opacity at the right lower lung lobe

Case Study 11

Fig. 20.19 SARS. At day 3 of the illness course, chest X-ray demonstrates wedge-shaped high-density shadow at the right upper lung lobe

Case Study 12

Fig. 20.20 SARS. At day 3 of the illness course, CT scanning demonstrates flakes of ground-glass opacity at the lateral basilar segment of the left lower lung lobe

Case Study 13

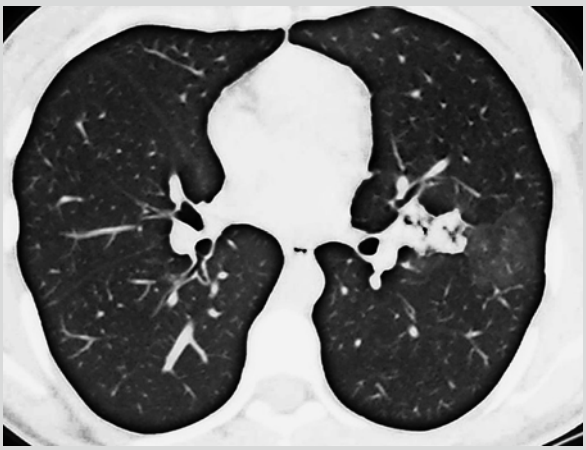

Fig. 20.21 SARS. At day 3 of the illness course, CT scanning demonstrates flakes of ground-glass opacity at the anterior lateral basilar segment of the left lower lung lobe and consolidation of some lesions

20.7.2 The Progressive Stage

Chest X-ray and CT scanning demonstrate the progressive stage of SARS as large flakes of shadows, which are multiple or diffuse. The lesions may expand from one lung lobe to multiple lung lobes and from one lobe at one lung to the other lung or both lungs. The ground-glass opacity at the early stage is demonstrated with increased density to consolidation. Otherwise, ground-glass opacities with different densities are concurrent with consolidation. The pulmonary vascular shadows at the affected lung are demonstrated to be increased and thickened (Figs. 20.22 and 20.23).

Case Study 14

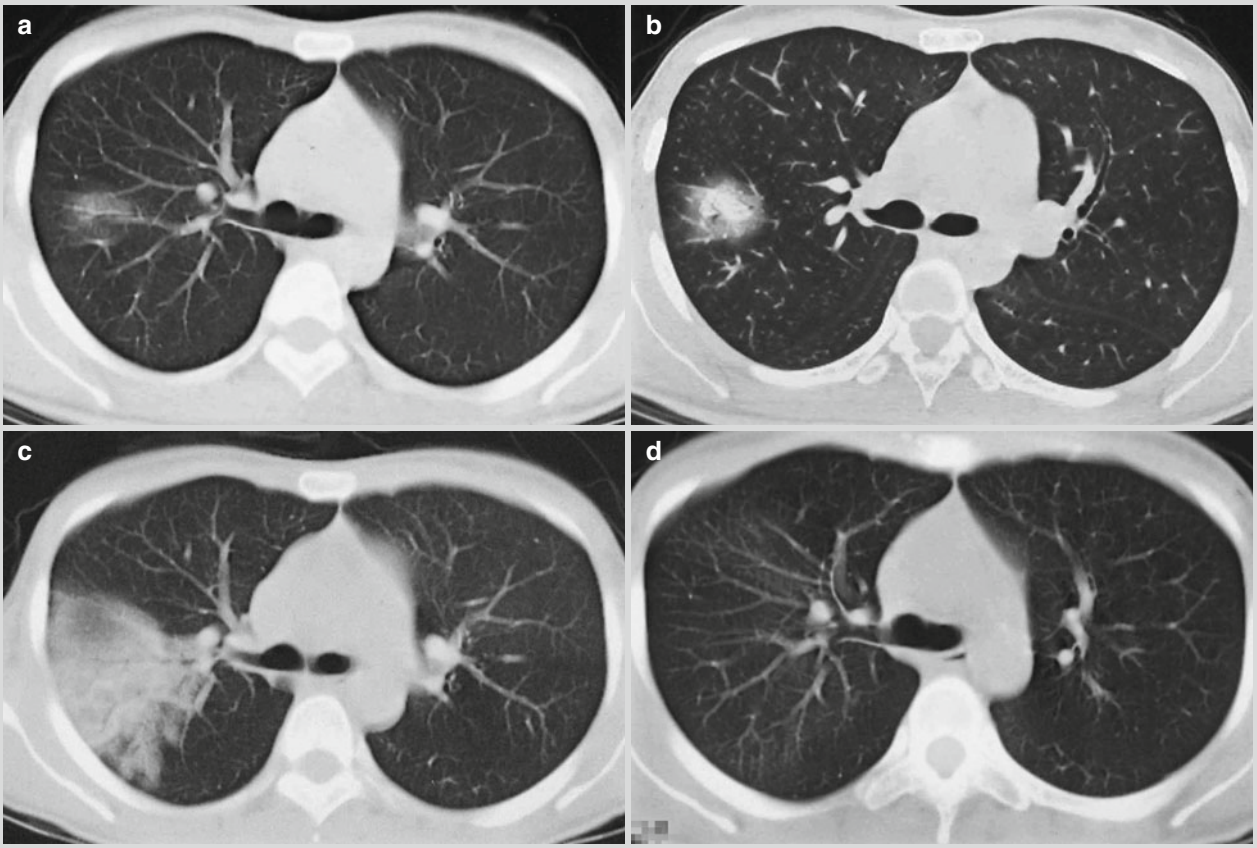

Fig. 20.22 SARS. (**a**) On the first day of the course, CT scanning demonstrates round-like ground-glass shadow in the right upper lung. (**b**) On the fourth day of the course, lesions' density increases and range expands. (**c**) On the 11th day of the course, lesions are characterized by large-sheet-shaped consolidation, with visible air bronchogram inside. (**d**) On the 16th day of the course, basically the absorption of lesions is displayed

Case Study 15

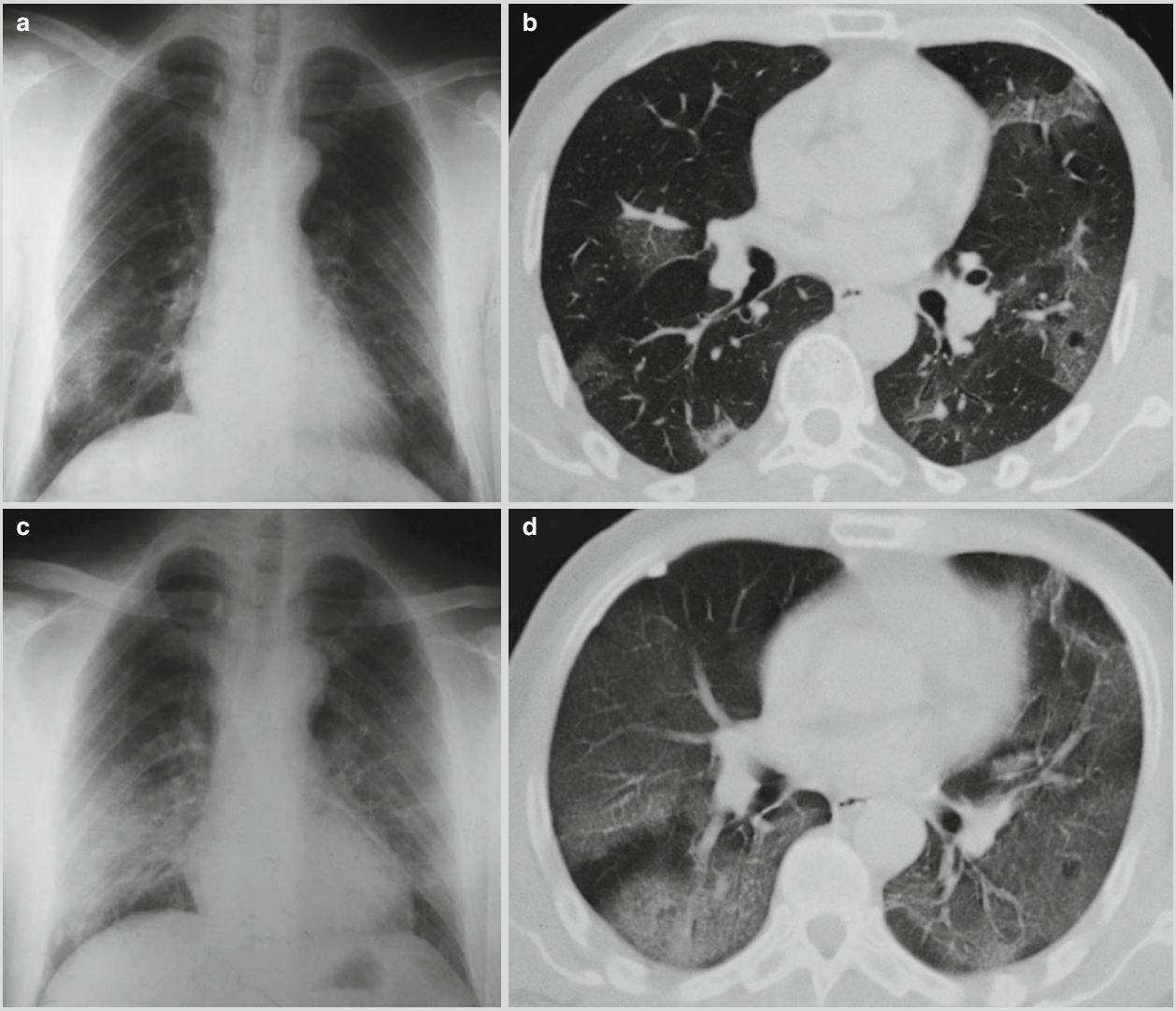

Fig. 20.23 SARS. (**a**) At day 3 of the illness course, chest X-ray demonstrates patches of shadows at both lower lungs. (**b**) CT scanning demonstrates multiple flakes of ground-glass shadows at both lower lungs. (**c**) At day 8 of the illness course, the lesions progress, demonstrated by chest X-ray with large flakes of shadows with increased density at the bilateral middle and inferior lungs. (**d**) CT scanning demonstrates diffuse ground-glass shadow at both lungs. (**e**) At day 12 of the illness course, chest X-ray demonstrates obvious absorption of large flakes of shadow with increased density at both lungs. (**f**) CT scanning demonstrates obvious absorption of ground-glass opacity at both lungs. (**g**) At day 17 of the illness course, chest X-ray demonstrates basically the complete absorption of lesions at both lungs. (**h**) At day 18 of the illness course, CT scanning demonstrates basically the complete absorption of ground-glass opacity at both lungs

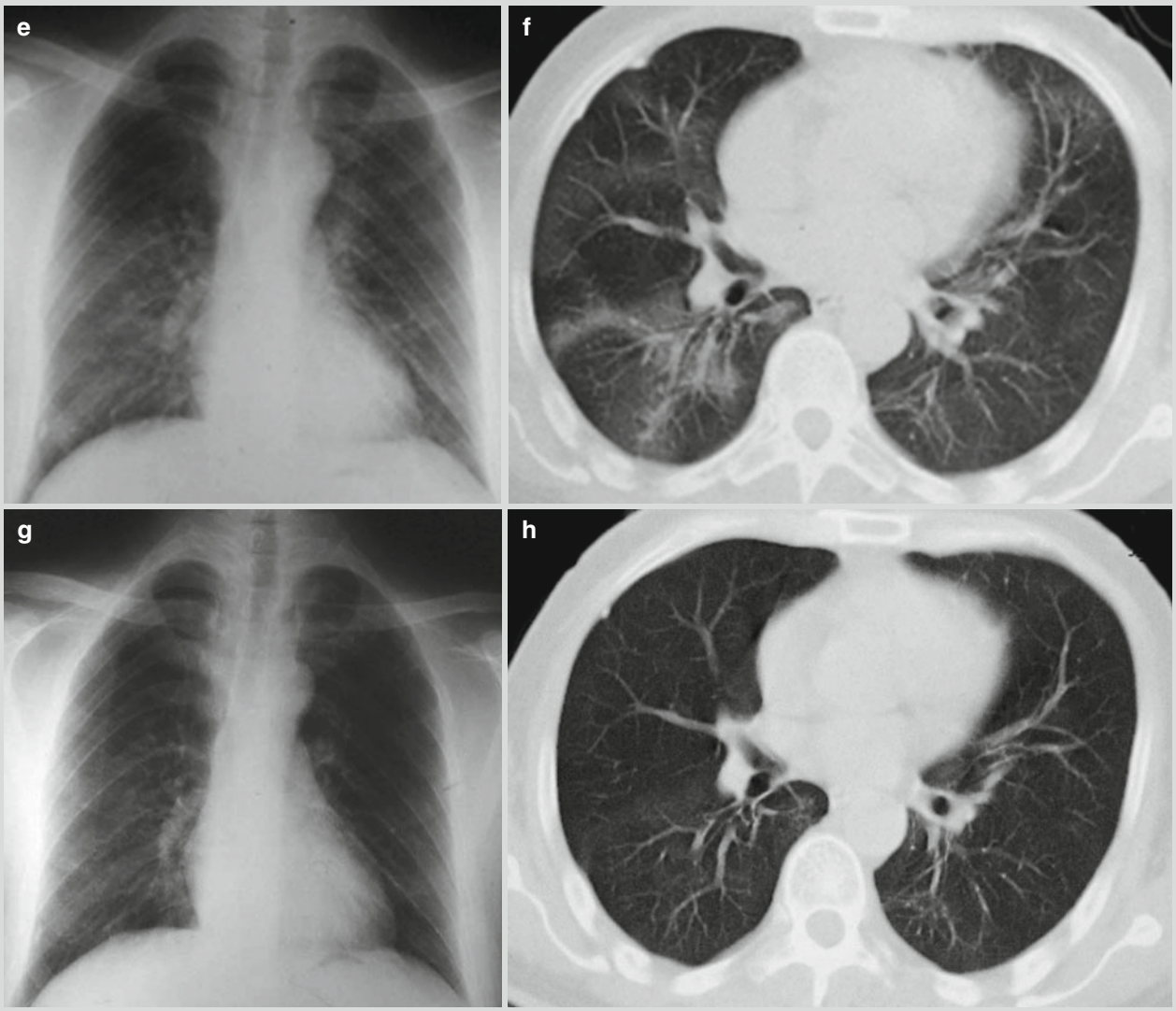

Fig. 20.23 (continued)

In some patients with SARS, the main radiological demonstration is interstitial exudation at the lungs, with honeycomb-like lung resembling pulmonary interstitial fibrosis and slight alveolar exudation (Figs. 20.24 and 20.25).

Case Study 16

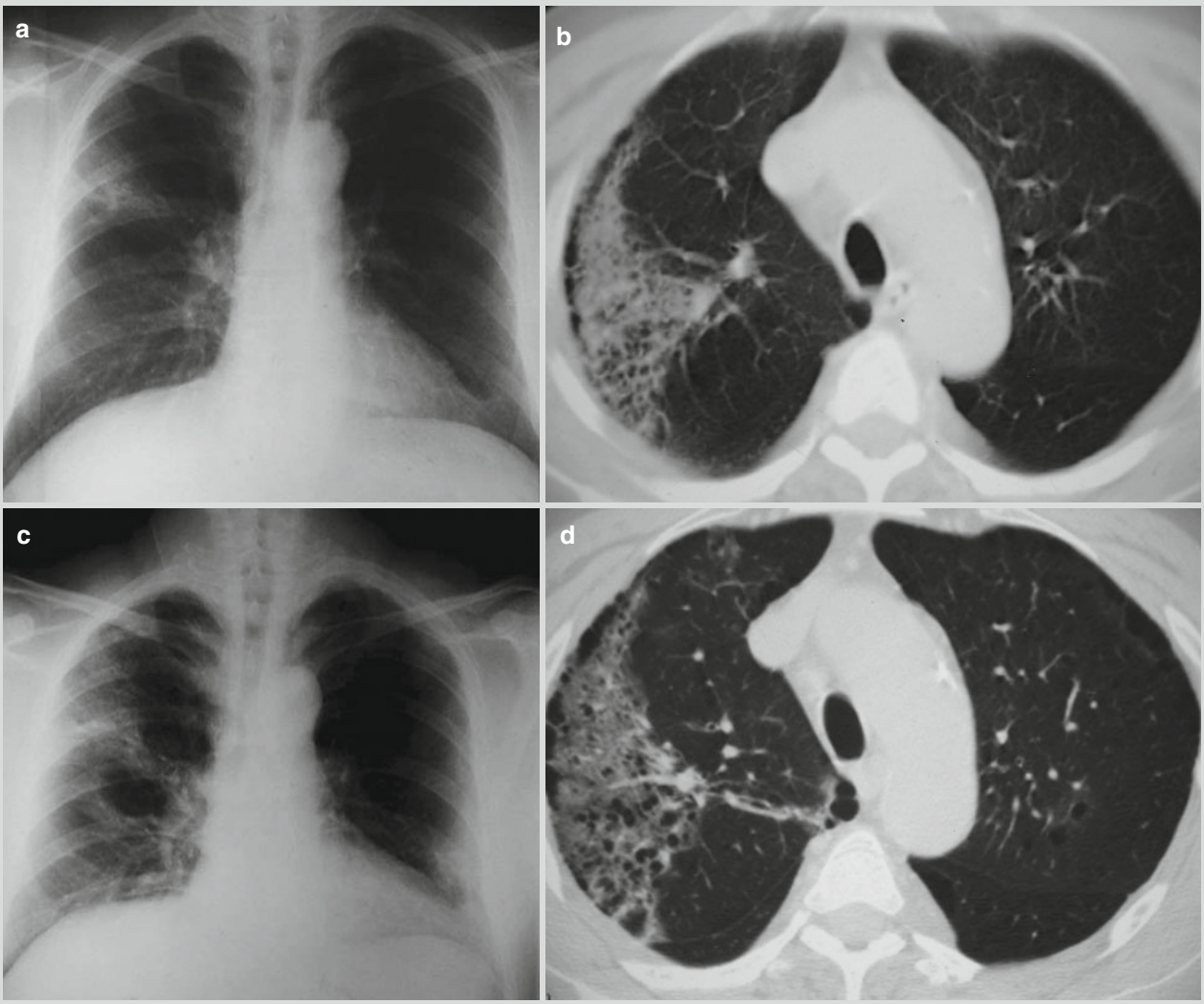

Fig. 20.24 SARS. (**a**) At day 7 of the illness course, chest X-ray demonstrates subpleural large flakes of shadows at the right middle and lower lung fields. (**b**) CT scanning demonstrates ground-glass opacity at the right lung with small honeycomb-like change. (**c**) At day 11 of the illness course, chest X-ray demonstrates expanded range with flakes of shadows under the pleura at the right lung. (**d**) At day 11 of the illness course, CT scanning demonstrates ground-glass opacity at the right lung with honeycomb-like change. (**e**) At day 14 of the illness course, CT scanning demonstrates shrinkage of the range with lesions and decreased density of the lesions

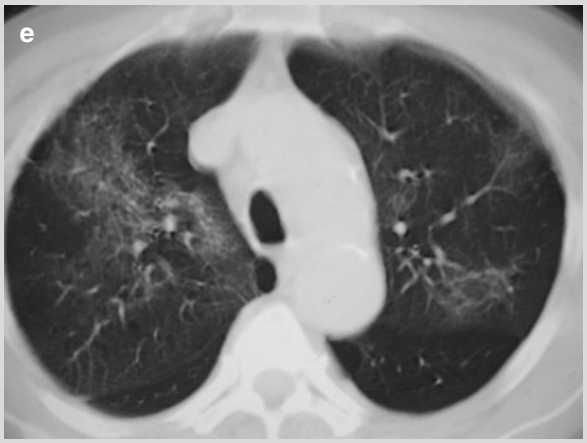

Fig. 20.24 (continued)

Case Study 17

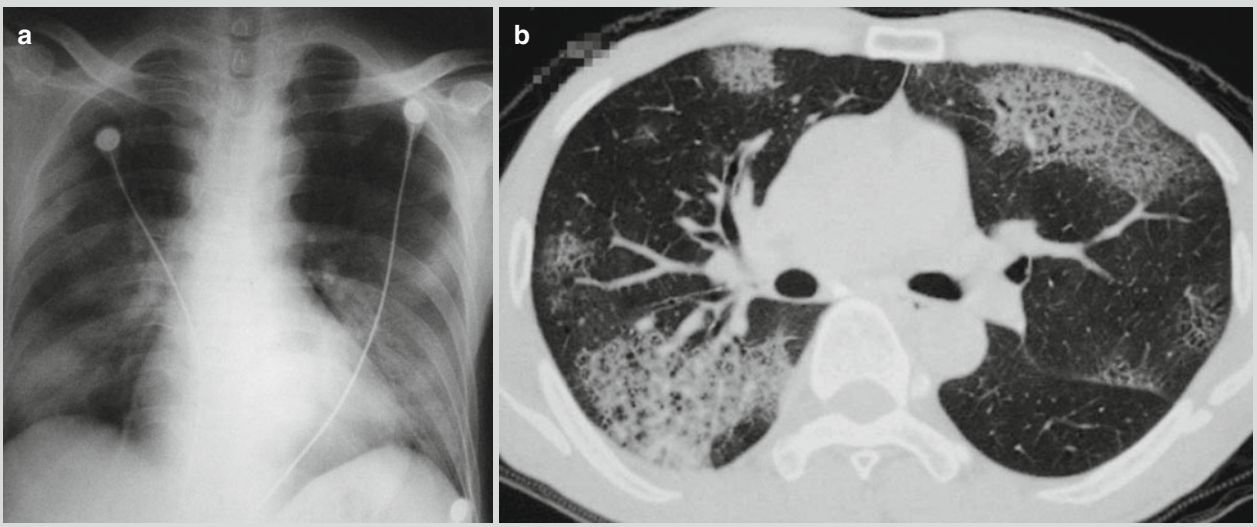

Fig. 20.25 SARS. (**a**) At day 7 of the illness course, chest X-ray demonstrates diffuse flakes of shadows with high density at both lungs. (**b**) CT scanning demonstrates multiple ground-glass opacities at both lungs with inner alveolar shadow, characterized by the paving stone sign. (**c**) At day 14 of the illness course, chest X-ray demonstrates obvious absorption of both pulmonary lesions. (**d**) At day 16 of the illness course, CT scanning demonstrates absorption and absence of ground-glass opacity at both lungs. (**e**) At day 25 of the illness course, chest X-ray demonstrates enhanced lung markings at the bilateral lower and middle lungs. (**f**) CT scanning demonstrates obvious absorption of ground-glass opacity at both lungs and local fiber cord-like shadow

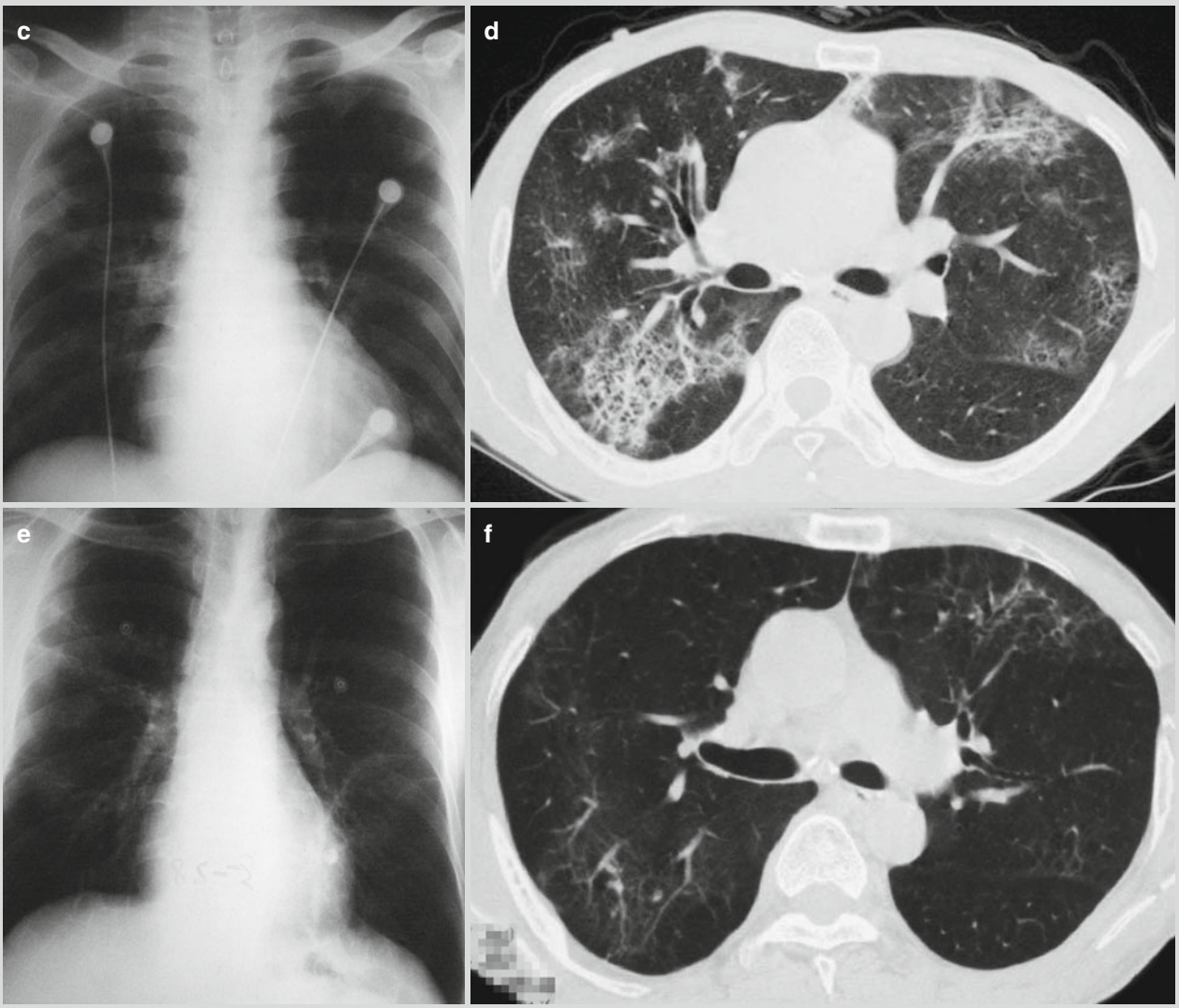

Fig. 20.25 (continued)

20.7.3 The Severe Stage

20.7.3.1 X-Ray Radiology

Both lungs are demonstrated with singular or multiple large flakes of shadows that rapidly develop into extensive or diffuse pulmonary consolidation, in white lung sign. Clinically, the patients experience respiratory distress syndrome. In rare patients, the lesions can be completely absorbed after treatment. The lesions are commonly located at the lower lobe of both lungs and under the pleura.

20.7.3.2 CT Scanning

(1) Large area of diffuse ground-glass opacity or pulmonary consolidation, (2) rapid progress of the lesions, (3) accompanying acute lung injury and ARDS (Figs. 20.26 and 20.27), and (4) secondary bacterial or fungal infections

Case Study 18

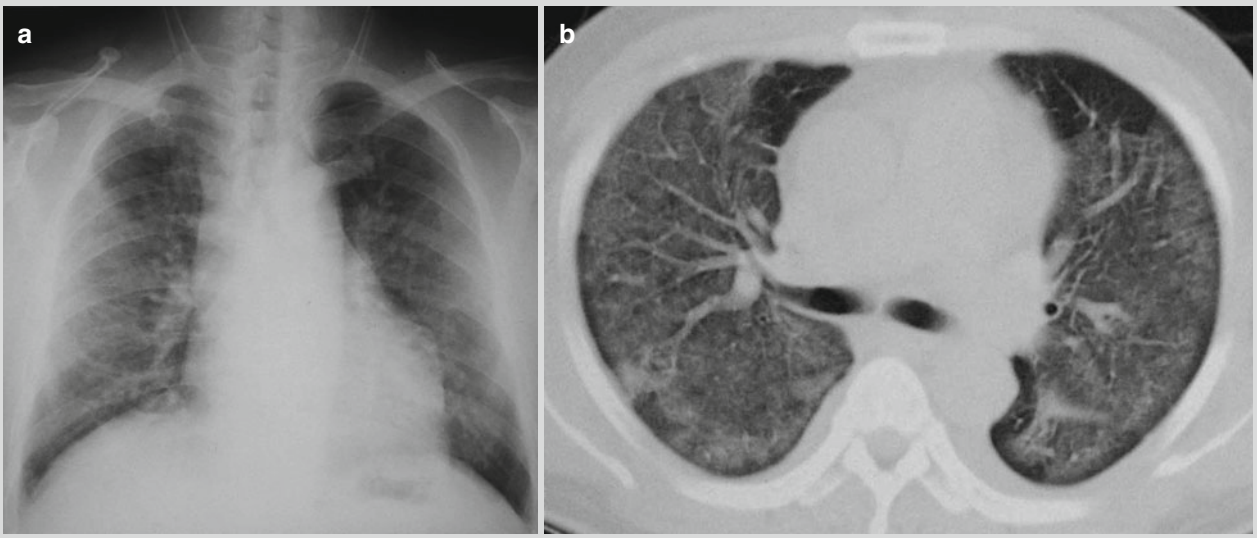

Fig. 20.26 SARS. (**a**) At day 9 of the illness course, chest X-ray demonstrates increased density at the bilateral lower and middle lung fields. (**b**) CT scanning demonstrates diffuse ground-glass opacity at both lungs

Case Study 19

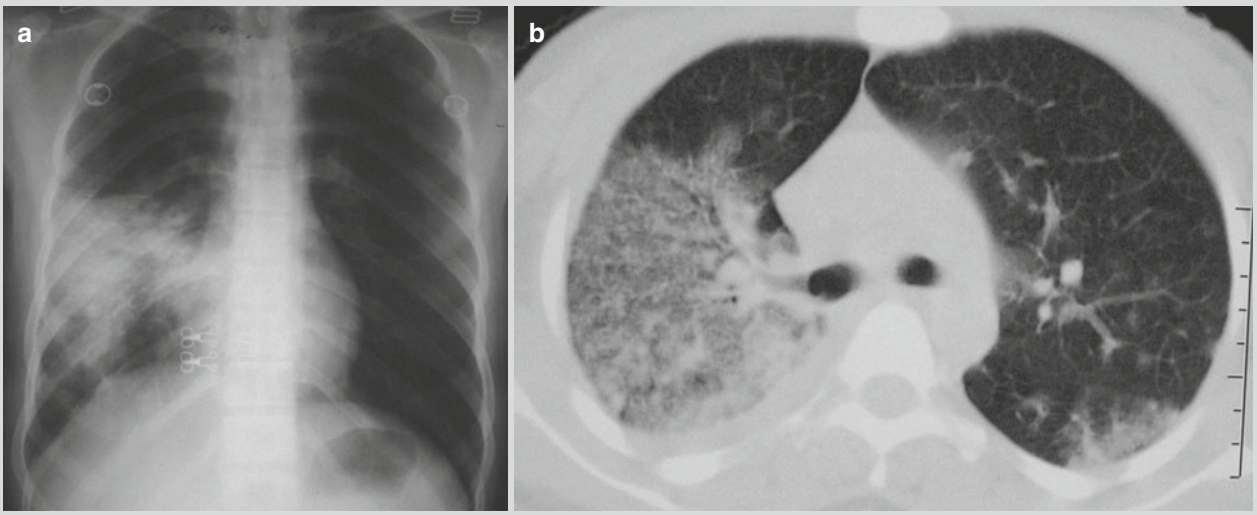

Fig. 20.27 SARS and ARDS. (**a**) At day 9 of the illness course, chest X-ray demonstrates large flake of shadow with high density at the right lower and middle lung fields. (**b**) CT scanning demonstrates ground-glass shadow at the right lung and dorsal segment of the left lower lung lobe, which is more obvious at the right lung. (**c**) At day 11 of the illness course, chest X-ray demonstrates white lung sign at the right lung and the left lower and middle lung fields. (**d**) CT scanning demonstrates diffuse ground-glass shadow and consolidation at both lungs. (**e**) Pathology demonstrates evenly light-stained acidophilic exudated fluid filled in the alveolar cavity that is serous or cellulosic fluid and formation of hyaline membrane by condensed exudates that adheres to the alveolar wall (H&E, ×200)

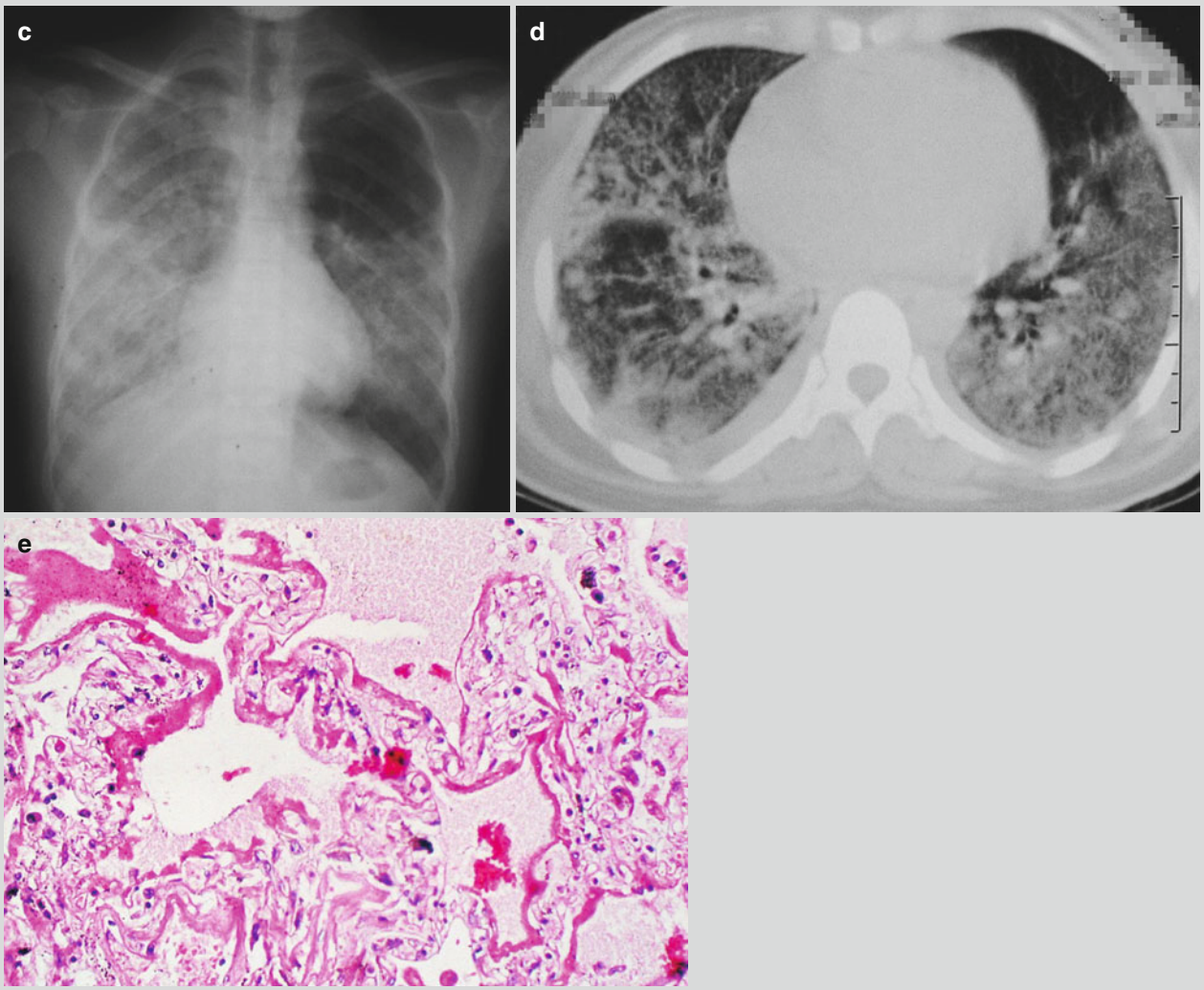

Fig. 20.27 (continued)

Chest X-ray and CT scanning demonstrate the non-characteristic shape of the lesions, which presents a challenge for its differential diagnosis from other pneumonia. However, the dynamic changes radiologically demonstrated are different from other pneumonia. By diagnostic imaging examinations, the shape and range of lung lesions are demonstrated with rapid changes, with obvious changes of size within 24 h. In some cases, new lesions at other locations can be demonstrated after absorption of the lesions at one location. In some cases, after obvious absorption of the lesions, repeated occurrence or aggravation of the lesions is demonstrated. In cases with aggravated lesions, the range with lesions is demonstrated to be enlarged, with occurrence of new lesions. In some other cases, the absorption of the lesions requires a longer period of time, which may be double or even longer compared to common lesions.

20.7.4 Radiological Demonstrations of SARS-Related Complications

The complications of SARS commonly occur during or after its progressive stage.

20.7.4.1 Secondary Infection

Pulmonary secondary infections (bacteria, fungi, tuberculosis, etc.) are important complications of SARS, which can lead to more lesions in enlarged range that persist for a longer period of time. During the convalescent stage of SARS, secondary lung infection can cause flakes of lesions to increase again. The secondary lung infection can also cause cavity and pleural effusions (Figs. 20.28 and 20.29), commonly 2–3 weeks after the onset. The cavity can be singular or multiple, whose pathogenic

diagnosis should be based on corresponding etiological test. In some patients, the complicating cavity and pleural effusions are found during follow-up reexamination after being discharged from the hospital. There are also some patients experiencing secondary brain infection. In the cases with symptoms and signs of the central nervous system, brain CT or MRI should be recommended for diagnosis.

Case Study 20

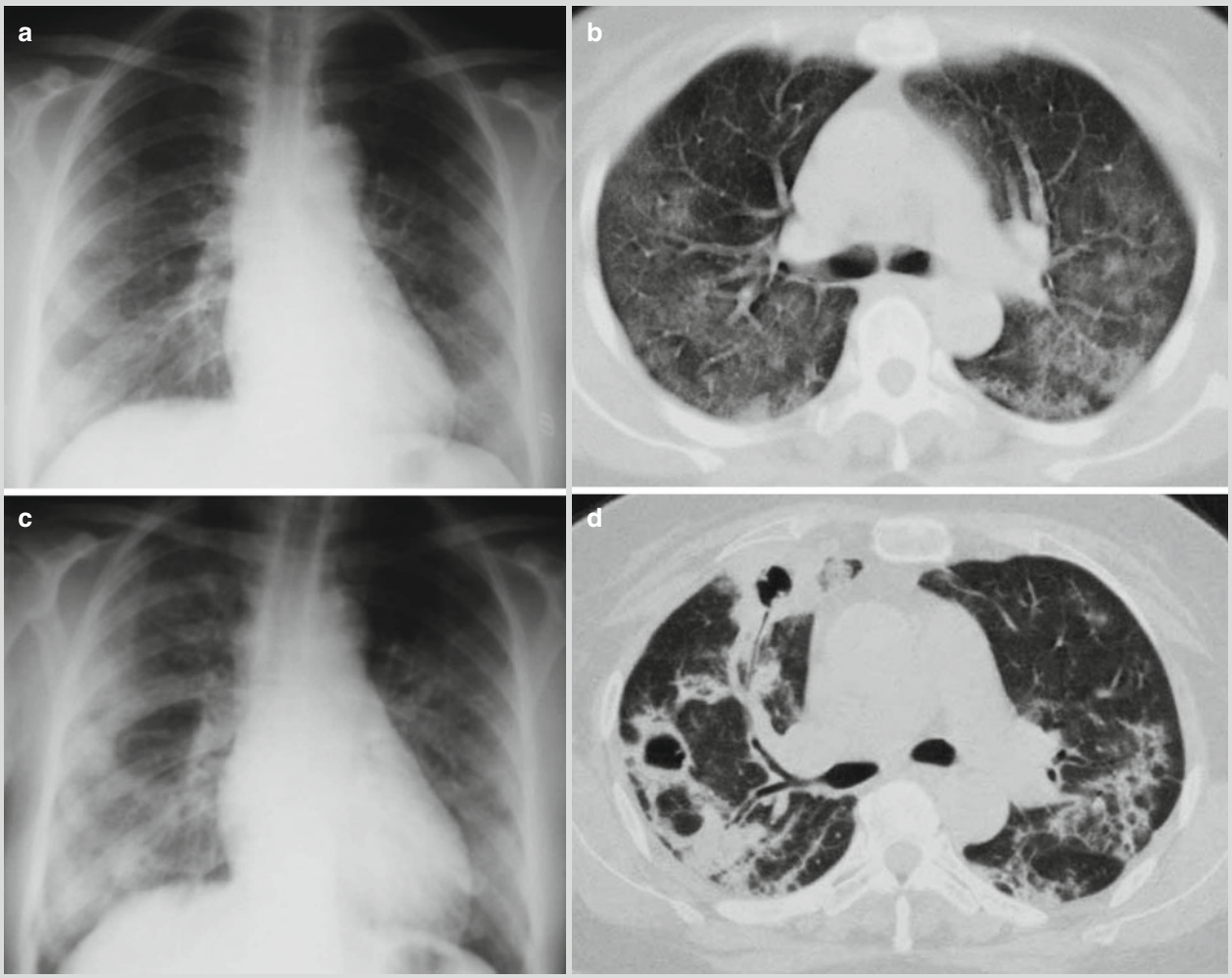

Fig. 20.28 SARS complicated by *Staphylococcus aureus* infection. (**a**) At day 16 of the illness course, chest X-ray demonstrates large flake of shadow with increased density at the bilateral lower and middle lung fields. (**b**) CT scanning demonstrates ground-glass opacity at both lungs. (**c**) At day 25 of the illness course, chest X-ray demonstrates progress of the lesions at both lungs and cavity at the right middle lung field. (**d**) CT scanning demonstrates pulmonary consolidation and multiple cavities at the right lung

Case Study 21

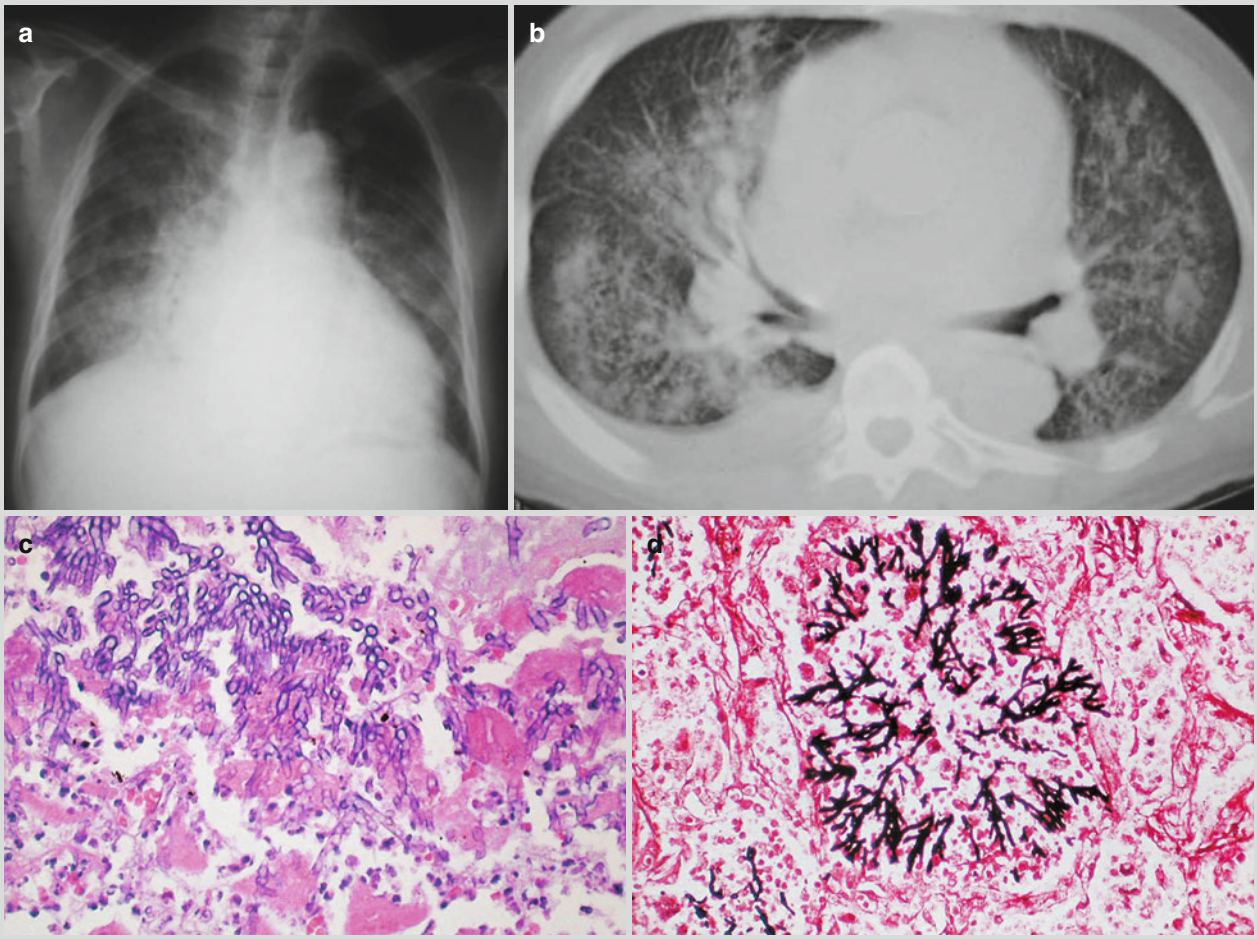

Fig. 20.29 SARS complicated by aspergillus infection. (**a**) At day 62 of the illness course, chest X-ray demonstrates multiple patches of shadows at both lungs and enlarged heart shadow. (**b**) CT scanning demonstrates enhanced lung markings at both lungs and patches of shadows along the lung markings. (**c**) Pathology demonstrates aspergillus infection at the lungs (H&E, ×400). (**d**) The lesion of aspergillus infection is stained black by methenamine silver staining (methenamine silver, ×400)

20.7.4.2 Pulmonary Interstitial Changes

In rare patients, residual pulmonary interstitial fibrosis can be found after absorption of intrapulmonary inflammation, characterized by localized irregular high-density patches of, cord-like, fine network of, and honeycomb-like shadows. These lesions may cause bronchiectasis (Fig. 20.30). Severe pulmonary interstitial hyperplasia can cause shrinkage of lung volume. The lesion of pulmonary interstitial fibrosis is radiologically demonstrated to be irreversible. During the absorption of inflammations, especially severe cases, chest X-ray may demonstrate enhanced lung markings and strips of shadows, which tend to be misdiagnosed as pulmonary interstitial fibrosis. By HRCT, thickened bronchovascular bundle can be demonstrated, with thickened interlobular septum and intralobular interstitial tissue as well as subpleural arch-shaped linear shadow. During rehabilitation, most of these changes can be gradually absorbed, but the absorption of some lesions requires a longer period of time.

Case Study 22

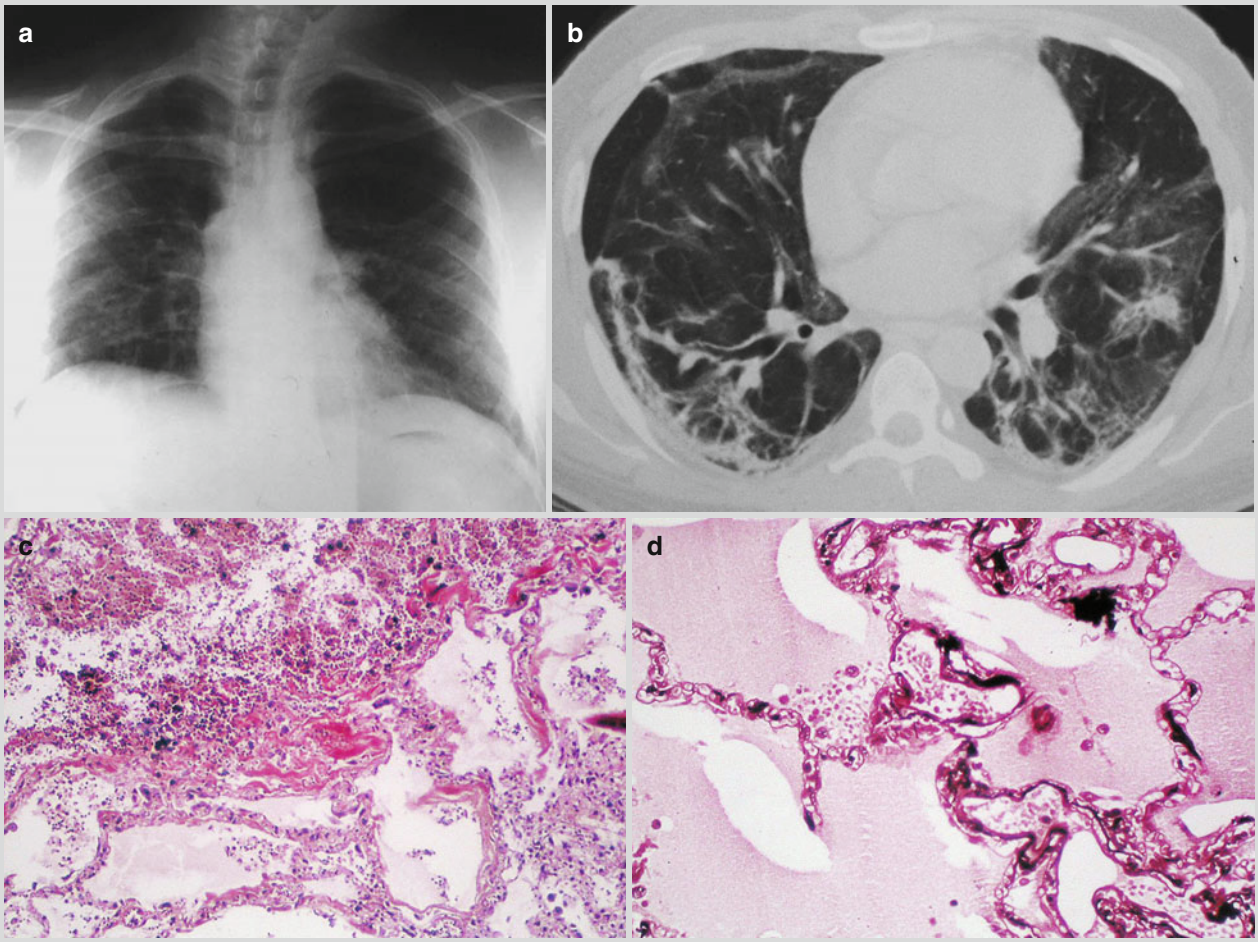

Fig. 20.30 SARS complicated by pulmonary interstitial changes. (**a**) At day 62 of the illness course, chest X-ray demonstrates enhanced lung markings at both lungs and fibrous cord-like shadow. (**b**) CT scanning demonstrates uneven density at both lungs and multiple cord-like shadows. (**c**) The alveolar capillary wall is subject to proliferation of reticular fiber to cause irregular thickening of the capillary wall (reticular fiber, ×200). (**d**) The alveolar septum is demonstrated with proliferation of collagen fiber to cause the rose color and irregular shape of the alveolar septum (PTAH, ×200)

20.7.4.3 Mediastinal Emphysema, Subcutaneous Emphysema, and Pneumothorax

Mediastinal emphysema is characterized by a strip or flake of gas shadow at the mediastinal space. The large gas shadow may be located around the esophagus, trachea, major vascular vessels, pericardium, and other structures (Fig. 20.31). Subcutaneous emphysema is obvious. Pneumothorax is demonstrated with small volume. In some cases, mediastinal emphysema, subcutaneous emphysema, and pneumothorax are demonstrated after the use of respirator.

Case Study 23

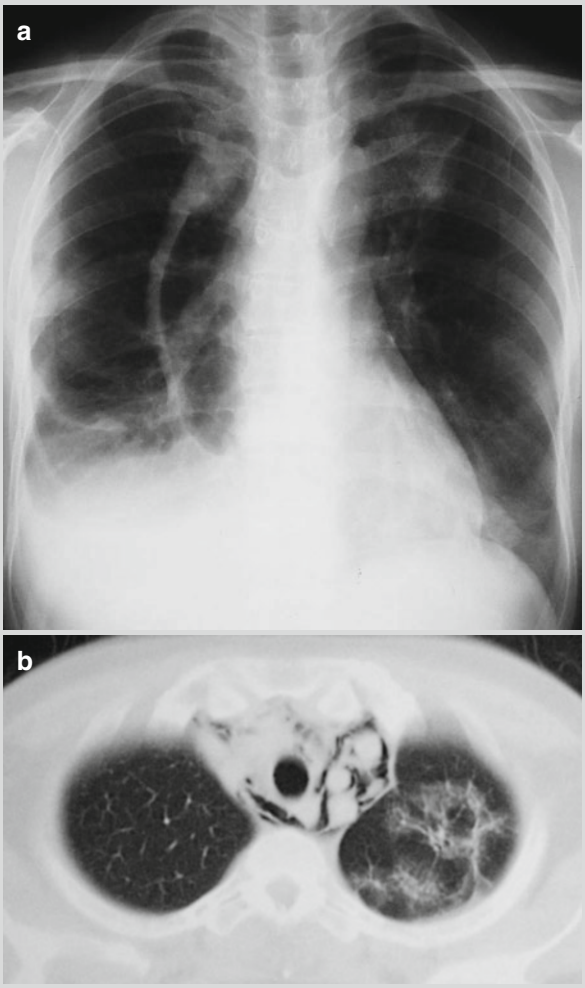

Fig. 20.31 SARS complicated by mediastinal emphysema. (**a**) X-ray demonstrates irregular transparent area in the mediastinum. (**b**) CT scanning demonstrates multiple gas density shadows in the mediastinum and multiple patches of and cord-like shadows at the left upper lung lobe

20.7.4.4 Pleural Lesions

Intrapulmonary lesions can involve the adjacent pleura to cause localized pleural thickening or slight curtain-like adhesion. The pleural changes can be absent along with absorption of intrapulmonary lesions. Obvious pleural effusion is rarely found.

20.7.4.5 Enlarged Heart Shadow

It may be caused by myocardial lesions. The size of heart shadow can be assessed based on standing anterior chest X-ray. By bedside chest X-ray, the effects of transverse heart and expanded heart shadow should be paid focused attention before assessment.

20.7.4.6 Bone Ischemia and Necrosis

After treatment, the patients may experience joint pain and confined movements, and CT scanning or MR imaging should be recommended for them. The bone changes are commonly demonstrated at the hip and knee joints. And the ankle, shoulder, and other joints as well as diaphysis of the long bone can also be involved (Fig. 20.32). Cheng XG et al. reported that the main bone change of SARS during rehabilitation is ischemic necrosis, whose MR imaging demonstrations are the following:

Ischemic Necrosis of the Femoral Head

Typical linear abnormal signal is demonstrated under the loaded articular surface of the femoral head, with low T1WI signal and obviously high STIR signal.

Ischemic Necrosis of Femoral Condyle

Bone necrosis underneath the articular surface of femoral condyle is demonstrated as linear or patches of abnormal signal under the articular surface of distal femoral condyle with commonly direct extension of both ends to the articular surface. The abnormal signal is low on T1WI and obviously high on STIR.

Bone Infarction

Bone infarction within the bone marrow is characterized by a large area of map-like abnormal signal at the bone marrow with no connection to the articular surface. The infarction area is demonstrated at the center of the lesion, with surrounding reactive area. The infarction area is demonstrated as high signal on T1WI and low signal on STIR. The reactive area is demonstrated as low signal on T1WI and obviously high signal on STIR.

Articular Cavity Effusion

Articular cavity effusion is demonstrated as obviously high signal on fat-suppressed T2WI. In addition, at its early stage, MR imaging demonstrates edema of the bone marrow.

Case Study 24

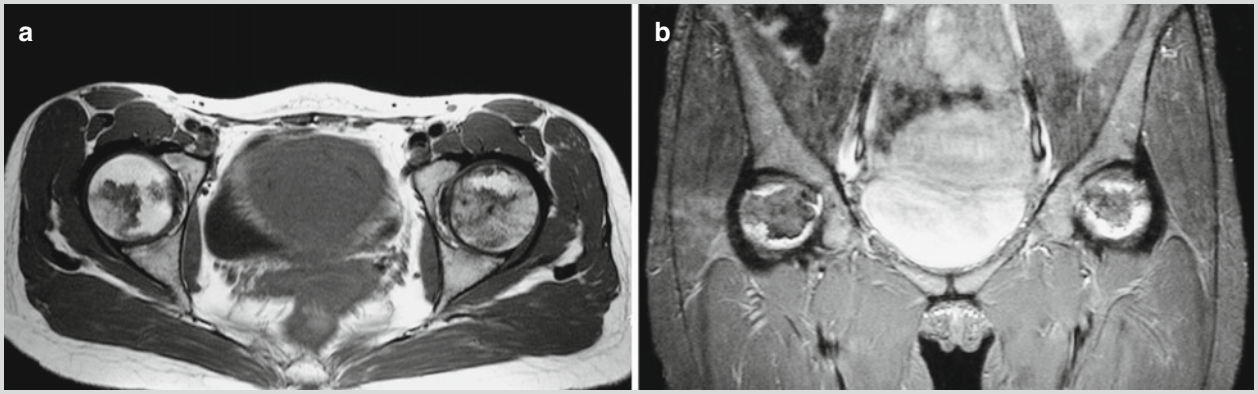

Fig. 20.32 SARS complicated by bone ischemia and necrosis. (**a**) Fat-suppressed T2WI demonstrates uneven signal at bilateral femoral heads, uneven flakes of equal signal and linear low signal in the high signal ring, and no deformity of the femoral head. (**b**) Coronal T1WI of the hip joint demonstrates linear low-signal area at the inferior femur and subchondral uneven low-signal area at the femoral joint

20.8 Diagnostic Basis

20.8.1 Diagnosis of SARS

Currently, the diagnosis of SARS is still based on clinical diagnosis. On April 14, 2003, the diagnostic criteria were established by the Ministry of Health, China, in combination of its epidemiology, clinical symptoms and signs, common laboratory tests, chest X-ray demonstrations, and responses to therapy.

20.8.1.1 Diagnostic Criteria of SARS Issued by the Ministry of Health, China

Epidemiological History

1. The patient has a history of close contact to patients with SARS, or is a member of an infected group, or has definite evidence to have infected others.
2. Within 2 weeks before the onset, the patient visited or lived in a city with reported cases of SARS or its secondary infection.

Symptoms and Signs

SARS has an acute onset, with fever as its initial symptom and a body temperature of above 38 °C and occasional aversion to cold. The patients may also experience accompanying headache, joint pain, muscular soreness, fatigue, and diarrhea, commonly without respiratory catarrhal symptoms. Cough may be clinically found, which is commonly dry cough with rare sputum or occasionally blood-stained sputum. Chest distress may be reported, and in some severe cases, the patients may experience rapid respiration, shortness of breath, or apparent respiratory distress. Pulmonary signs are not obvious, and in some patients, rare moist rales can be heard or pulmonary consolidation can be found.

Laboratory Tests

The peripheral blood WBC count is commonly normal or decreased, and the count of lymphocytes is commonly decreased.

Chest X-Ray

At the lungs, varying degrees of flakes and patches of infiltrative shadows or grid-like shadows are demonstrated. In some cases, the lesions progress rapidly, with large flake of shadow. In most cases, the lesions are bilaterally found, with slow absorption. The shadows demonstrated at the lungs may be inconsistent with clinical symptoms and signs. The cases demonstrated negative by chest X-ray should receive reexaminations after 1–2 days.

Antibacterial Medication

By treatment of antibacterial drugs, the therapeutic efficacy is not obvious.

The criteria for suspected cases should be in accordance with above 1 + 2 + 3 or 2 + 3 + 4. And the criteria to define the diagnosis should be in accordance with above 1 (1) +2 + 4 or 1 (2) + 2 + 3 + 4 or 1 (2) + 2 + 4 + 5.

20.8.1.2 Diagnostic Criteria of Severe SARS

Cases of SARS with one of the following conditions can be defined as severe SARS:

1. Dyspnea, with a respiratory rate above 30 times/min;
2. Hypoxemia, after inhaling oxygen at 3–5 L/min, with the arterial partial pressure of oxygen lower than 70 mmHg or pulse volume of blood oxygen saturation lower than 93 %; otherwise, the cases can be diagnosed with acute lung injury or acute respiratory distress syndrome;
3. Multilobar lesions with a range exceeding one-third of the lung; otherwise, chest X-ray demonstrates progress of lesions above 50 % within 48 h;
4. Shock or multiple organ dysfunction syndrome;
5. The patient sustains severe fundamental disease or complication of other infections above the age of 50 years.

20.8.2 Diagnosis of SARS-Related Complications

20.8.2.1 Secondary Infection

SARS complicated by secondary infection is demonstrated by chest X-ray with more lesions in a larger range that persist for a longer period of time as well as accompanying cavity and pleural effusions. The diagnosis can be defined based on etiological test.

20.8.2.2 Pulmonary Interstitial Changes

After absorption of intrapulmonary inflammation in patients with SARS, chest X-ray demonstrates localized irregular patches of, cord-like, fine network of, and honeycomb-like shadows with high density and bronchiectasis. The severe cases may also be demonstrated with shrinkage of lung volume. By HRCT, the demonstrations include thickened bronchovascular bundle, thickened interlobular septum and intralobular interstitial tissue, and subpleural arch-shaped linear shadow.

20.8.2.3 Mediastinal Emphysema, Subcutaneous Emphysema, and Pneumothorax

In cases of SARS, the patients may experience chest distress and retrosternal pain, with dilated jugular vein, tachycardia, and dyspnea. By physical examination, the subcutaneous tissue is swollen, with spongy feeling and crepitant rale as well as the sensation of treading on snow by touch. By auscultation, clicking sound at heartbeat can be heard at the precordial region. Chest X-ray demonstrates strip or flake of gas shadow at the mediastinal space and beneath the skin. The large gas shadow can be located around the esophagus, trachea, major vascular vessels, and pericardium. In cases complicated by pneumothorax, the patients experience sudden chest pain, following chest distress or dyspnea, and irritated dry cough. Chest X-ray demonstrates no lung markings at the area of pneumothorax and compressed lung margin.

20.8.2.4 Pleural Lesions

Chest X-ray demonstrates localized pleural thickening or slight curtain-like adhesion. The pleural lesions can be absent after absorption of intrapulmonary lesions.

20.8.2.5 Bone Ischemia and Necrotic Changes

After receiving cholesterol therapy, the patients with SARS experience joint pain and confined movements. The cases with demonstrated confined abnormal signal at the femoral head, accompanying low or equal marginal signal, and/or double linear sign by MR imaging can be defined as ischemia and necrosis of the femoral head.

20.9 Differential Diagnosis

In clinical practice, SARS should be differentiated from traditional atypical pneumonia (caused by mycoplasma, legionella, chlamydia, and rickettsia) and typical pneumonia (lobar and lobular pneumonia), viral pneumonia, interstitial pneumonia, allergic pneumonia, pulmonary edema, pulmonary atelectasis, pulmonary tuberculosis, and lung cancer. The diagnosis of SARS is based on exclusion, which can hardly be qualitatively diagnosed based on radiological demonstrations. However, its diagnosis should be comprehensively based on epidemiologic history, clinical demonstrations, laboratory tests, and chest radiological examination. Hereby, the clinical manifestations and imaging demonstrations of several respiratory diseases with commonalities with SARS are briefly described as the following:

20.9.1 Other Virus Pneumonia

The radiological demonstrations of virus pneumonia are almost the same as those of SARS. By chest X-ray, the lesions are characterized by singular or multiple patches and large flakes of shadows, diffusely increased density shadows at unilateral or bilateral lungs, and local or bilateral enhanced lung markings. CT scanning demonstrates ground-glass opacity or consolidation shadow (Figs. 20.33 and 20.34). The definite diagnosis is commonly based on etiological test.

Case Study 25

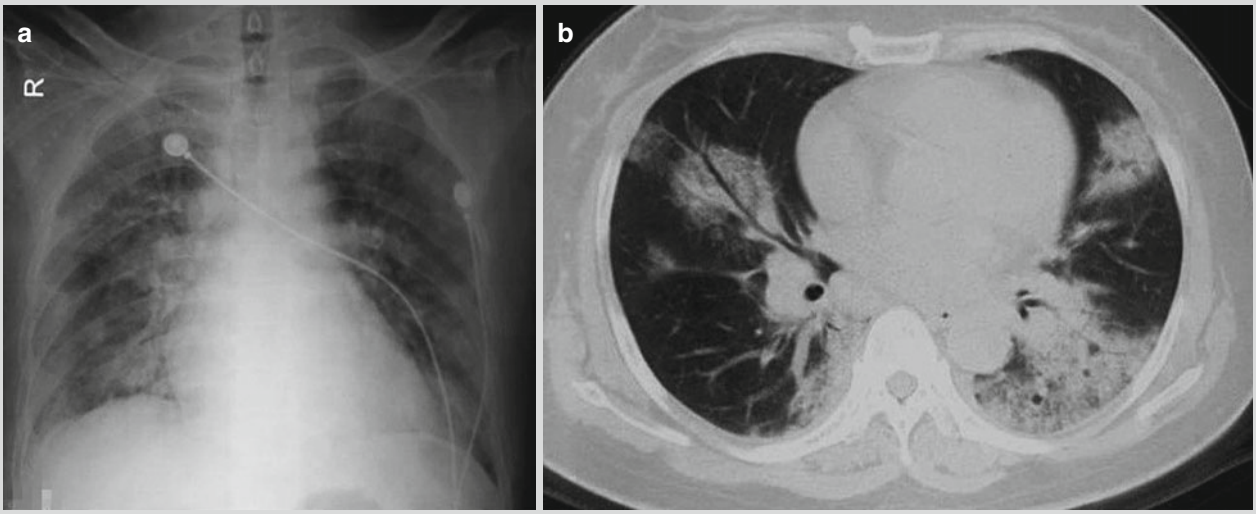

Fig. 20.33 Influenza virus pneumonia. (**a**) X-ray demonstrates patches of blurry shadows at both lungs. (**b**) CT scanning demonstrates multiple ground-glass opacities and consolidated shadow

Case Study 26

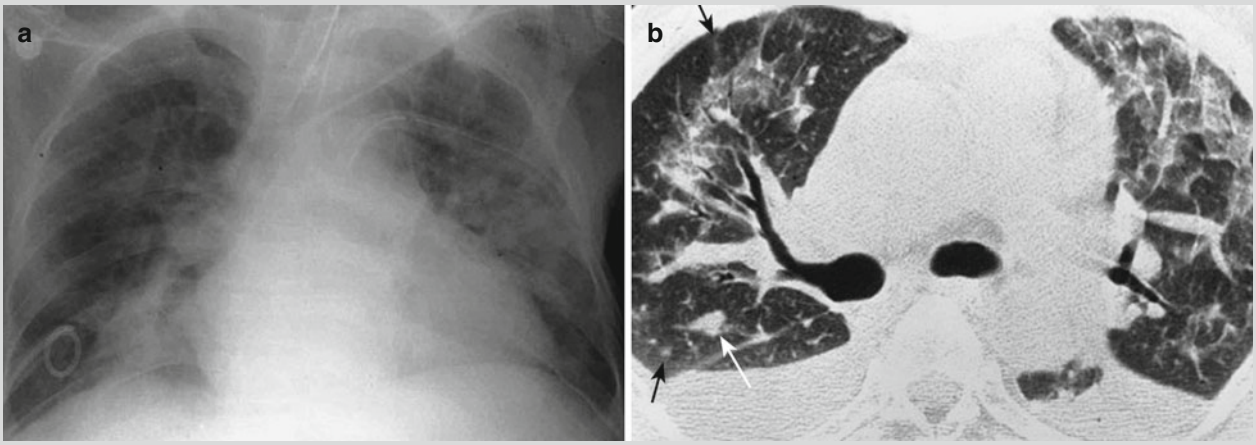

Fig. 20.34 CMV pneumonia. (**a**) X-ray demonstrates patches of blurry shadows at both lungs. (**b**) CT scanning demonstrates ground-glass opacity (*black arrows*), nodules (*white arrow*)

20.9.2 Mycoplasma Pneumonia

Chest X-ray demonstrates increased lung markings and polymorphic infiltrative shadows at the pulmonary parenchyma that are more common at the lower lung lobe. The infiltrative lesions can also be demonstrated as spots, patches, or homogeneous blurry shadows (Fig. 20.35). In about one-fifth of patients, pleural effusion can be demonstrated in a small quantity. The definitive diagnosis is based on positive finding by streptococcus MG agglutination test, detection of serum antigen and antibody, and/or PCR detection of mycoplasma DNA.

Case Study 27

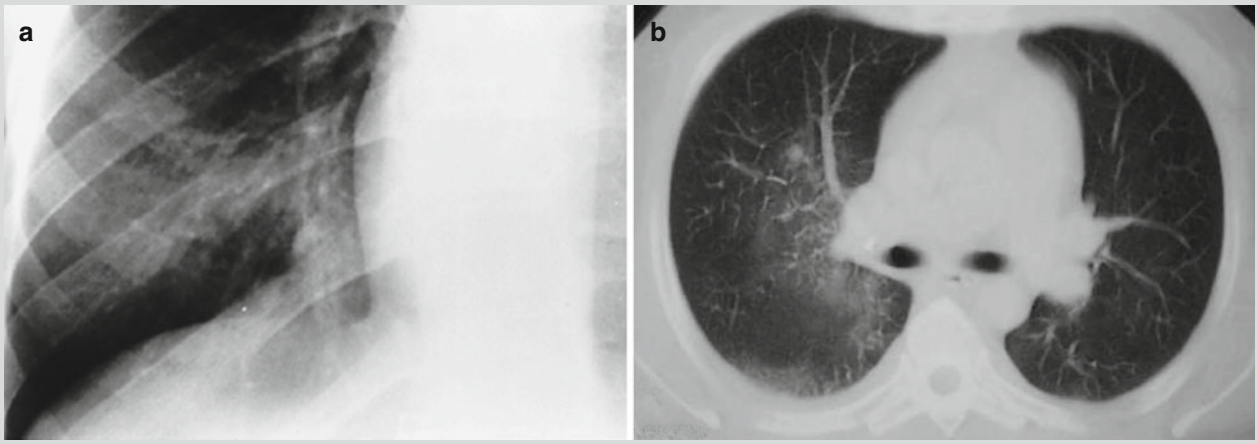

Fig. 20.35 Mycoplasma pneumonia. (**a**) X-ray demonstrates enhanced lung markings and patches of blurry shadows at the right lower lung. (**b**) CT scanning demonstrates ground-glass shadow at the right lung

20.9.3 *Pneumocystis carinii* Pneumonia (PCP)

It commonly occurs in people with compromised immunity, such as patients with advanced AIDS, middle-aged and elderly people, individuals with malnutrition, and patients with cancer receiving chemotherapy. It is characterized by acute onset with symptoms of fever, dry cough, rare expectoration, and dyspnea. X-ray demonstrates diffuse ground-glass opacity or grid-like shadow at both lungs, predominantly interstitial lesions (Figs. 20.36 and 20.37). It can be hardly differentiated from severe SARS. In combination with case history, especially those receiving immunosuppressants, the diagnosis can be made.

Case Study 28

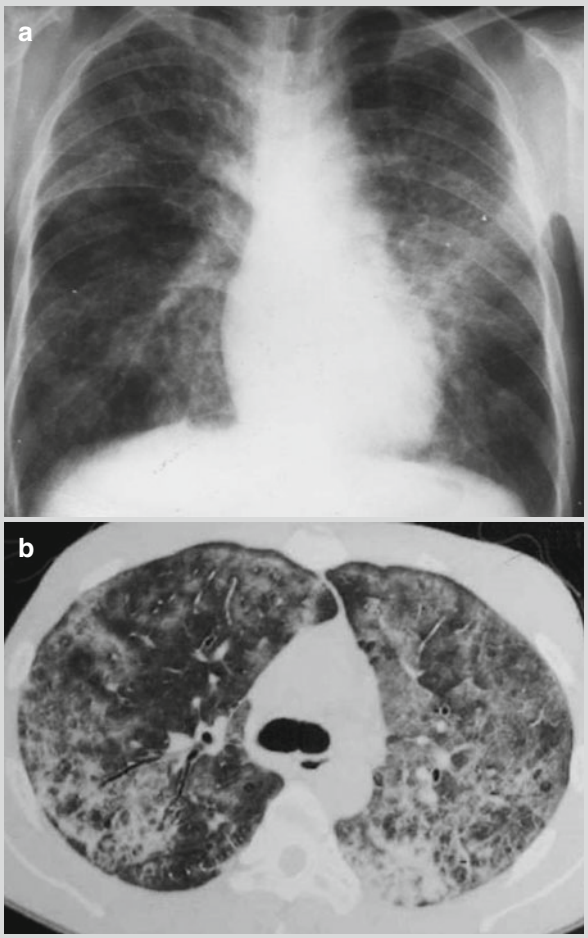

Fig. 20.36 PCP. (**a**) X-ray demonstrates grid-like and cord-like shadows at both lungs and accompanying diffusely increased density. (**b**) CT scanning demonstrates ground-glass shadows at both lungs

Case Study 29

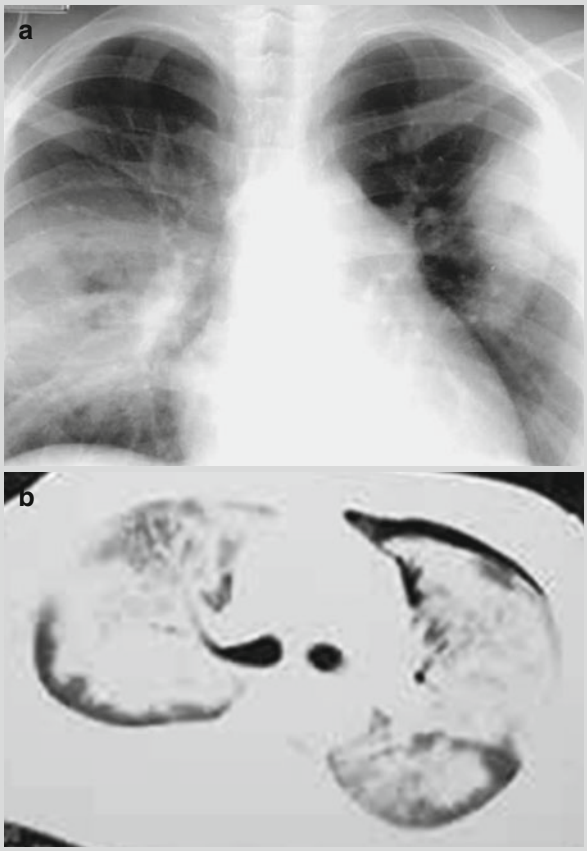

Fig. 20.37 PCP and pneumothorax. (**a**) X-ray demonstrates large flakes of shadows with increased density in both lungs. (**b**) CT scanning demonstrates ground-glass opacity and consolidation shadows at both lungs and left pneumothorax

20.9.4 Legionella Pneumonia

X-ray demonstrates common patches of shadows, which are nonspecific. In severe cases, multiple lung lobes are involved, rarely with formation of cavities. The lesions at the lungs can be absorbed within 1–2 months, being slower than absorption of lung lesions in cases of common pneumonia. It is characterized by progress of lung lesions by chest X-ray while the patients are receiving effective therapies. In some cases, complications may occur, such as pericarditis, myocarditis, endocarditis, acute renal failure, shock, and DIC.

20.9.5 Fungal Lung Infection

It commonly occurs in persons with compromised immunity, such as patients with AIDS or diabetes. In recent years, due to large-dose use of antibiotics, hormone, cytotoxic drugs, and immunosuppressants, the incidence of fungal lung infection has been increasing. Chest X-ray demonstrates diverse nonspecific lesions, which might be bronchopneumonia, lobar pneumonia, diffuse small nodular shadows, or mass-like shadows (Fig. 20.38).

Case Study 30

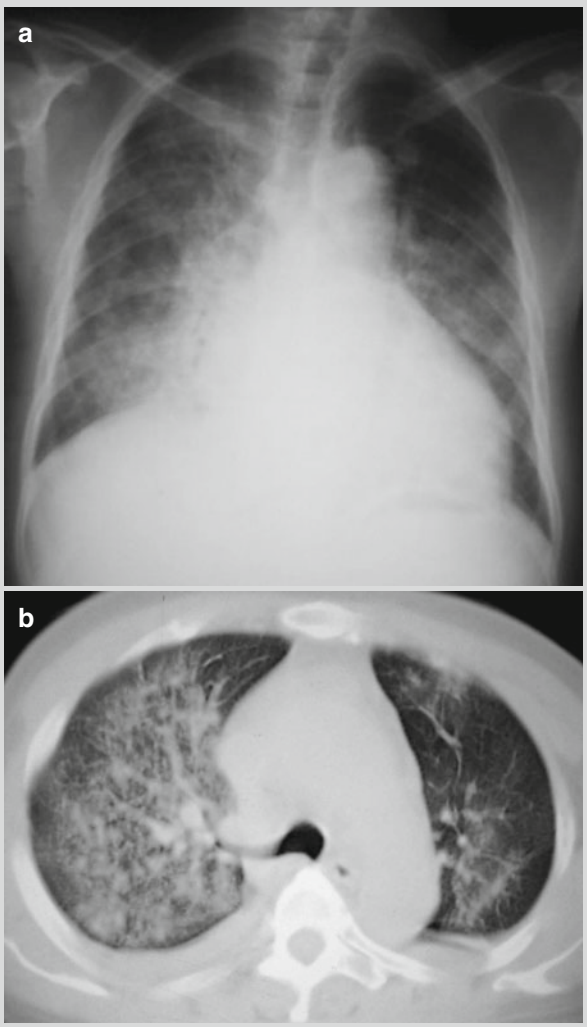

Fig. 20.38 Pulmonary fungal infection. (**a**) X-ray demonstrates enhanced lung markings in both lungs, patches of shadows along lung markings, and enlarged heart shadow. (**b**) CT scanning demonstrates the consolidation of both lungs, especially the right lung

Further Reading

Chen XG, Qu H, Liu W, et al. Screening of bone ischemic necrosis for its incidence rate in rehabilitating patients with severe acute respiratory syndrome by MR imaging. Chin J Radiol. 2005;39(8):791–7.

Lang ZW, Zhang LJ, Zhang SJ, et al. Autopsy and pathological analysis of 3 death cases of severe acute respiratory syndrome. Chin J Pathol. 2003;32(3):201–4.

Lee N, Hui D, Wu A, et al. A major outbreak of severe acute respiratory syndrome in Hong Kong. N Engl J Med. 2003;1348(20):1986–94.

Liang LC, Li TY. Clinical staging of SARS and the radiological demonstrations. Clin Pearls. 2003;18(22):1282–3.

Liu JX, Tang XP. Atalas of chest radiology for diagnosis of SARS (case review). Beijing: Science Press; 2003.

Lu PX, Zhou BP, Gong XL, et al. Chest x-ray demonstrations of severe acute respiratory syndrome. J Clin Radiol. 2003;22(6):449–51.

Nicolaou S, Al-Nakshabandi NA, Müller NL. SARS: imaging of severe acute respiratory syndrome. AJR Am J Roentgenol. 2003; 180(5):1247–9.

Wang W, Ma DQ, Zhao DW, et al. CT scanning demonstrations and their dynamic changes of SARS. Chin J Radiol. 2003;37(8):686–9.

Wang W, Zhang XZ, Lu Y, et al. Bone ischemic necrosis in SARS patients after hormonal therapy by MR imaging. Chin J Radiol. 2004;38(3):236–9.

Wong KT, Antonio GE, Hui DS, et al. Thin-section CT of severe acute respiratory syndrome: evaluation of 73 patients exposed to or with the disease. Radiology. 2003;228(2):395–400.

Xu DH, Jia CY, Li CQ, et al. Radiological demonstrations and pathological analysis of death cases from SARS. Chin J Radiol. 2004;38(5):455–8.

Yuan CW, Zhao DW, Wang W, et al. Imaging demonstrations of intrapulmonary cavity in the cases of SARS. Chin J Radiol. 2004;38(5):466–9.

Zhang XZ, Wang W, Lu Y, et al. CT scanning demonstrations of chest and complications of SARS. Chin J Radiol. 2003;37(9):775–9.

Zhang TK, Zhang K, Wang SZ, et al. Dynamic changes of T cell and its subpopulation in 95 cases of SARS. J Capital Univ Med Sci. 2004;25(3):338–40.

Zhao CH. Practical studies of SARS. Beijing: People's Medical Publishing House; 2003.

Zhao DW, Ma DQ, Wang W, et al. Early X-ray and CT scanning demonstrations of severe acute respiratory syndrome. Chin J Radiol. 2003;37(7):597–9.